ADVANCED REVIEW

WIREs CLIMATE CHANGE WILEY

Variability and long-term change in Australian monsoon rainfall: A review

Hanna Heidemann[1,2] | Tim Cowan[1,3] | Benjamin J. Henley[4,5,6,7] |
Joachim Ribbe[2] | Mandy Freund[3,8] | Scott Power[1,7,9]

[1]Centre for Applied Climate Sciences, University of Southern Queensland, Toowoomba, Queensland, Australia

[2]School of Sciences, University of Southern Queensland, Toowoomba, Queensland, Australia

[3]Bureau of Meteorology, Melbourne, Victoria, Australia

[4]Securing Antarctica's Environmental Future, University of Wollongong, Wollongong, New South Wales, Australia

[5]School of Earth, Atmospheric and Life Sciences, University of Wollongong, Wollongong, New South Wales, Australia

[6]Department of Infrastructure Engineering, University of Melbourne, Parkville, Victoria, Australia

[7]ARC Centre of Excellence for Climate Extremes, Monash University, Clayton, Victoria, Australia

[8]CSIRO Natural Environments, Melbourne, Victoria, Australia

[9]School of Earth, Atmosphere and Environment, Monash University, Clayton, Victoria, Australia

Correspondence
Hanna Heidemann, Centre for Applied Climate Sciences, University of Southern Queensland, Toowoomba, Queensland, Australia.
Email: hanna.heidemann@usq.edu.au

Funding information
De-Risk International Climate Initiative; Northern Australia Climate Program; University of Southern Queensland; Meat and Livestock Australia, the Queensland Government through the Drought and Climate Adaptation Program

Edited by: Mike Hulme, Editor-in-Chief

Abstract

The Australian monsoon delivers seasonal rain across a vast area of the continent stretching from the far northern tropics to the semi-arid regions. This article provides a review of advances in Australian monsoon rainfall (AUMR) research and a supporting analysis of AUMR variability, observed trends, and future projections. AUMR displays a high degree of interannual variability with a standard deviation of approximately 34% of the mean. AUMR variability is mostly driven by the El Niño-Southern Oscillation (ENSO), although sea surface temperature anomalies in the tropical Indian Ocean and north of Australia also play a role. Decadal AUMR variability is strongly linked to the Interdecadal Pacific Oscillation (IPO), partially through the IPO's impact on the strength and position of the Pacific Walker Circulation and the South Pacific Convergence Zone. AUMR exhibits a century-long positive trend, which is large (approximately 20 mm per decade) and statistically significant over northwest Australia. The cause of the observed trend is still debated. Future changes in AUMR over the next century remain uncertain due to low climate model agreement on the sign of change. Recommendations to improve the understanding of AUMR and confidence in AUMR projections are provided. This includes improving the representation of atmospheric convective processes in models, further explaining the mechanisms responsible for AUMR variability and change. Clarifying the mechanisms of AUMR variability and

change would aid with creating more sustainable future agricultural systems by increasing the reliability of predictions and projections.

This article is categorized under:

Paleoclimates and Current Trends > Modern Climate Change

1 | INTRODUCTION

There are eight tropical monsoon systems on Earth, providing water for over two-thirds of the world's population (Wang et al., 2021). Four of them are located across Asia/Australasia, two in the Americas and two in Africa. The majority of fresh water for the sparsely populated northern Australia (north of ~20° S, see black rectangle in Figure 1) comes from Australian monsoon rainfall (AUMR, Nicholls et al., 1982). Approximately 80% of the region's annual rainfall occurs during December to March (Suppiah, 1992). The AUMR is integral to northern Australia's ecology and biodiversity (Bowman, 2002), livestock (Cobon et al., 2019; McKeon et al., 2021), and cropping (Everingham et al., 2008; Meinke & Stone, 2005; Mollah & Cook, 1996; Suppiah, 1992).

The origin of the Australian monsoon (AUM) is most similar to that of the North African monsoon (Nie et al., 2010), as both arise from the seasonal migration of the Intertropical Convergence Zone (ITCZ) and the associated meridional shift in the overturning (Hadley) circulation, leading to a strong rainfall seasonality. From 60° E to the Dateline, the area of maximum rainfall varies by up to 20° latitude between austral winter (June to August, JJA) and austral
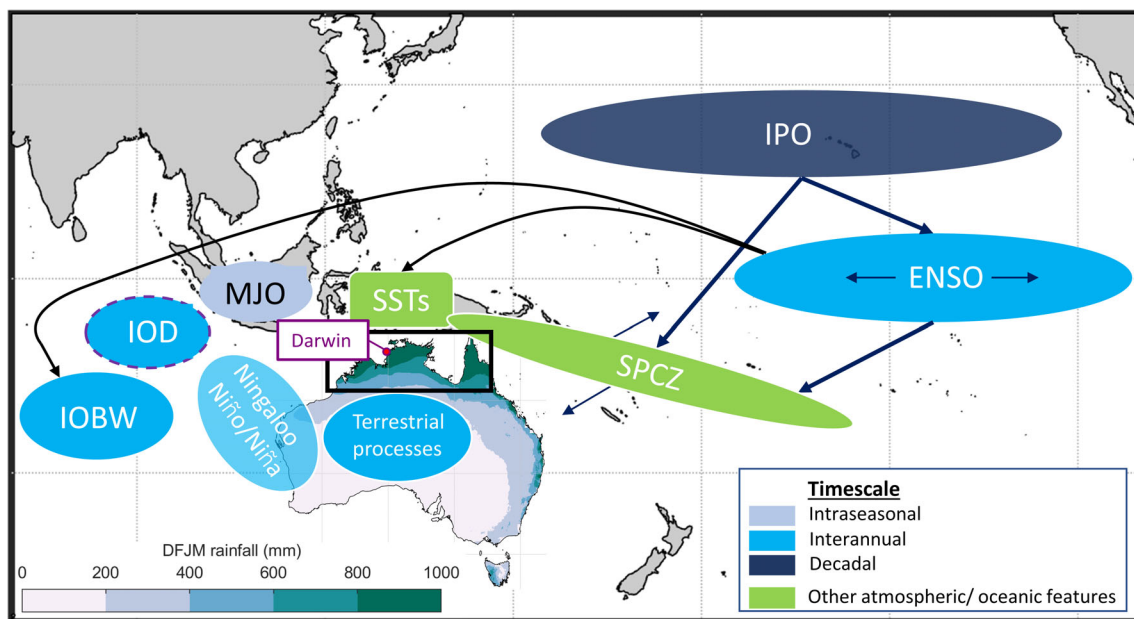
FIGURE 1 The main climate drivers and processes that influence Australian monsoon rainfall (AUMR) variability on different timescales. The AUMR region is indicated by the black rectangle and includes the Australian land area north of 20° S. Dashed lines indicate a lagged relationship between the driver and AUMR variability. Light green shading highlights atmospheric or oceanic features that influence AUMR variability. The mean accumulated rainfall from December to March is shown for Australia (1920–2021) using data from the Australian Water Availability Project (AWAP) dataset (Jones et al., 2009). A red dot indicates the location of Darwin, Northern Territory (12.4° S, 130.9° E). Acronyms: DJFM, December to March; ENSO, El Niño-Southern Oscillation; IOBW, Indian Ocean Basin-wide Warming; IOD, Indian Ocean dipole; IPO, Interdecadal Pacific Oscillation; MJO, Madden-Julian Oscillation; SPCZ, South Pacific Convergence Zone; SSTs, sea surface temperatures. Ningaloo Niño/Niña refers to SST anomalies off Australia's west coast.

summer (December to February, DJF). In summer, the strong rising motion around 10°S indicates the position of the ITCZ and is associated with large-scale deep convection and rainfall (Gadgil, 2018). A second, more shallow circulation flows from the subtropics toward the ITCZ region, with a branch of rising motion in the lower troposphere located pole-ward of the deep convection. This ascending air occurs over the Australian continent at approximately 23°S with peak potential temperatures in the boundary layer that coincide with meridionally broader rainfall maximums than would be expected by the ITCZ alone (Nie et al., 2010).

The AUM lies near the Indo-Pacific warm pool area (sea surface temperatures [SSTs] >28°C; Roxy et al., 2019), which attracts the ITCZ as it tends to follow the warm SSTs (Gadgil, 2018). The warm pool region is characterized by strong large-scale atmospheric upward motion that is associated with low-level convergent winds from the Indian and Pacific Oceans. This rising air forms the main ascending branch of the Walker Circulation, which further supports the existence and location of the AUM (Lau & Yang, 2003). Hence, the AUM is not entirely dependent on the land-ocean contrast (Chao & Chen, 2001).

There have been several important reviews on the climatology, dynamics, and variability of the AUM on intra-seasonal to interannual timescales. For example, the interannual relationship between the El Niño-Southern Oscillation (ENSO) and AUMR was well established by the early 1990s (Suppiah, 1992). Around the same time, the importance of intraseasonal drivers such as the Madden-Julian Oscillation (MJO) was emerging (Hendon & Liebmann, 1990a; Madden & Julian, 1994). Advances in the 2000s uncovered the importance of the MJO phase on the timing of AUM active and break periods (Wheeler & Hendon 2004), as well as the existence of convectively coupled equatorial waves (Kiladis et al., 2009). These advances in understanding were followed by a comprehensive review of the climatology and intraseasonal variability of the AUM (Wheeler & McBride, 2011). In the mid-2000s, Zhang and Moise (2016) provided a review of the representation of the AUM in climate models in the past, present-day, and future projections, drawing on results from the Coupled Model Intercomparison Project (CMIP) phases 3 (CMIP3) and 5 (CMIP5). Zhang and Moise (2016) concluded that there is a large spread between models in representing the climatological features of the AUM, and that model skill needs to be improved. More recently, Dey, Lewis, Arblaster, and Abram (2019) reviewed long-term trends in Australian rainfall during pre-instrumental and instrumental periods (Dey, Lewis, Arblaster, & Abram, 2019). They highlighted the existence of a positive trend in summer rainfall over northwest Australia. Since then, there has been a concerted effort to better understand and contextualize the onset of the AUM (Lisonbee et al., 2020). Their analysis showed that 25 different methods are used to define the AUM onset, and that the onset date varies markedly depending on which method is used.

To date, there has been no specific review focusing on decadal variability of AUMR. Hence, the purpose of this review is to update what is known about the interannual and decadal drivers of Australian monsoon rainfall variability (AUMRV, Figure 1) and we identify where gaps in our understanding of AUMRV and change remain. The paper is organized as follows: Section 2 provides the characteristics of the AUM, Section 3 discusses interannual AUMRV and associated mechanisms, while Section 4 focuses on decadal AUMRV and updates observed AUMR trends. Section 5 is focused on the representation of AUMR and its projected future change in coupled climate models. The main results are summarized in Section 6. Major research gaps and recommendations for increasing understanding are highlighted in Section 7. A description of the data and methods employed in this review is presented in Appendix S1.

2 | CHARACTERISTICS OF THE AUSTRALIAN MONSOON

Generally spanning December to March (DJFM), the AUM is often defined over northern Australia using rainfall (Jourdain et al., 2013), zonal winds (Kajikawa et al., 2010) or a combination of the two. Onset is indicated by a reversal of winds in the lower troposphere (e.g., 850 hPa) from easterly to westerly over the city of Darwin (Figure 1), equator-ward of the monsoon trough or ITCZ (Drosdowsky, 1996; Hendon & Liebmann, 1990b; Holland, 1986) and often trig-gered by the MJO (Hung & Yanai, 2004; Kawamura et al., 2002). The winds reverse from easterly pre-onset to westerly post-onset (Figure 2a,b). At the same time, a deepening of the monsoon trough over northwest Australia and enhanced precipitation over northern Australia and the Timor, Banda and Arafura Seas occurs (Figure 2c,d). The warm SSTs to the north of Australia during the pre-onset months play an important role for generating convective instabilities that favor the AUM onset (i.e., they are highly correlated to northern Australian rainfall; Hendon et al., 2012). Once the AUM commences, the SSTs in the Timor and Arafura Sea cool as a result of westerly wind stress, enhanced evaporation and cloudiness (Kawamura et al., 2002), and the SST-rainfall correlation breaks down (Hendon et al., 2012).
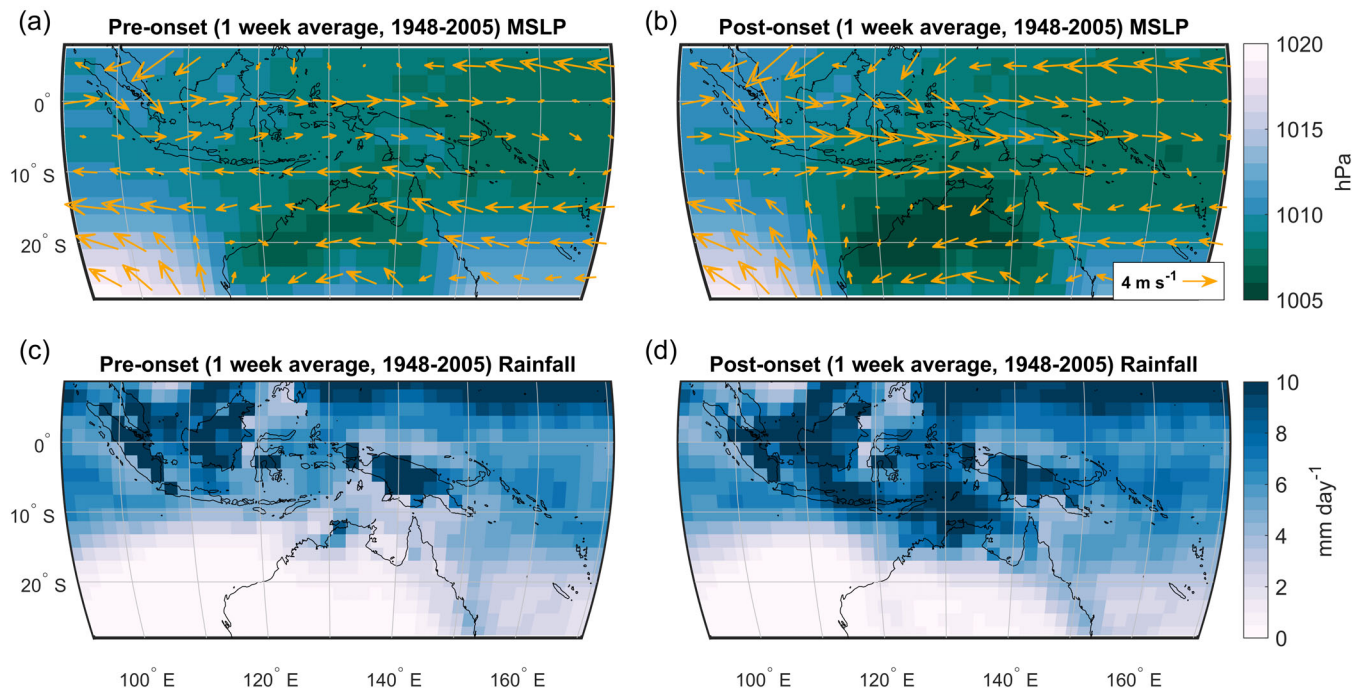
FIGURE 2 Atmospheric conditions during the week prior to (a,c) and post (b,d) onset of the Australian monsoon based on observations from 1948 to 2005. Shown are mean sea level pressure (MSLP, shading), 850 hPa winds (arrows) (a,b) and rainfall (c,d). Onset dates obtained are described in Appendix S1. Daily data for all displayed variables are taken from the NCEP/NCAR reanalysis version 1 dataset (Kalnay et al., 1996).

The winds associated with the AUM onset can be in the form of westerly bursts. These are short (>2 days) periods of intense (>5 m s^{-1}) westerlies that extend across the western Pacific (Sullivan et al., 2021). The wind bursts are accompanied by several consecutive rain days (Moise et al., 2020), which are interspersed by break periods of easterly anomalies that dampen convection (Troup, 1961). The cycle of rainfall (and accompanying wind) bursts and break periods is usually observed between late December and the AUM retreat in mid-March (Drosdowsky, 1996; Hendon & Liebmann, 1990b; Holland, 1986; Pope et al., 2009). The onset, retreat, and accumulated AUMR are highly variable on intraseasonal (Moise et al., 2020; Wheeler & McBride, 2007), interannual to multiyear (Sharmila & Hendon, 2020), and decadal timescales (Meehl & Arblaster, 2011).

While northern Australian rainfall bursts peak between mid-November and mid-December (Berry & Reeder, 2016), peak AUMR occurs in DJF (e.g. Kajikawa et al., 2010; Nagaraju et al., 2018; Narsey et al., 2020; Wang et al., 2004) and can extend into March (Cowan, Wheeler, Sharmila, Narsey, & de Burgh-Day, 2022). In this review, we describe the AUMR over the extended summer season (DJFM) for the Australian land region north of 20° S (Narsey et al., 2020) over the period January 1920 to March 2021. In contrast to the AUM season, the northern Australian wet season runs from November to April (Ghelani et al., 2017). We exclude higher latitude AUM definitions (Ashok et al., 2014; Marshall & Hendon, 2015) that encompass desert regions as identified by the Köppen vegetation class.[1] Similar to studies that use terrestrial rainfall (e.g. Jourdain et al., 2013), we divide the AUM region into northwest and northeast Australia at 135° E. Northwest Australia (NW) is a sparsely populated area that has experienced significantly wetter summers since the early 20th century (Dey, Lewis, Arblaster, & Abram, 2019), while northeast Australia (NE) is a region strongly influenced by ENSO (Sharmila & Hendon, 2020; Webster et al., 1998). Both are impacted by the MJO, which in turn can combine with ENSO during austral spring to enhance or weaken the intraseasonal rainfall signal (Lim et al., 2021). In contrast, rainfall over northern Australia during convective MJO phases appears to be less affected by ENSO during summer (Cowan, Wheeler, & Marshall, 2023).

To summarize, the key characteristics of the AUM are (1) an onset around late December that is often triggered by the MJO, (2) burst periods of westerly winds and rainfall during the monsoon season interspersed by break periods, and (3) a retreat around mid-March.

3 | AUMR: INTERANNUAL VARIABILITY

Before we review links between large-scale climate drivers and AUMR, we firstly characterize its variability. The left panels of Figure 3 show statistics that characterize interannual AUMRV such as the standard deviation and coefficient of variation. AUMR has a high degree of interannual variability, as indicated by the standard deviation (σ) being 34% of the mean (μ) AUMR (780 mm). Northern Australia and the eastern seaboard show the highest absolute σ, but the lowest coefficient of variation ($C_v = \sigma/\mu$) for DJFM rainfall, in comparison to the higher C_v but lower σ in central, southern, and western Australia (Figure 3a,c). The C_v over northern Australia is much higher in the drier austral winter months (Mollah & Cook, 1996). AUMRV is of similar magnitude to variability in rainfall over much of the continent, as far south as the southern Murray–Darling Basin (Figure 3e). About 28% of interannual AUMRV is associated with oceanic variability in the tropical Pacific and Indian Oceans ($R^2 = 0.28$ obtained by multiple linear regression [MLR]). This largely arises from the oceanic link with NE AUMR (26%; Table 1) as the link with NW AUMR is weaker (18%; Table 1). Compared to the Asian, African and American monsoon regions, the AUM appears to exhibit the highest coefficient of variation (Figure 3g). In monsoon regions, the C_v is generally lower in the Northern Hemisphere than the Southern Hemisphere (Figure 3g).

Oceanic feedback processes increase rainfall variability by approximately 30% over Australia, a finding based on a comparison between ocean–atmosphere coupled and atmospheric-only model simulations (Taschetto et al., 2016). Noting the mentioned study relied on a single model with known variability and equatorial Pacific biases (Taschetto et al., 2014), it nonetheless suggests the majority of interannual variability in AUMR is driven by nonoceanic variability. This includes internal atmospheric variability and atmosphere–terrestrial feedbacks.

In the following sections, we review the Indo-Pacific climate processes and feedbacks that influence AUMR on interannual timescales focusing on ENSO (Section 3.1), Indian Ocean modes of variability (Section 3.2), as well as terrestrial processes and internal atmospheric processes (Section 3.3).

3.1 | ENSO and AUMR interannual variability

ENSO has a strong imprint over northern and eastern Australia (Forootan et al., 2016; Sharmila & Hendon, 2020). Nevertheless, the state of ENSO makes little difference to rainfall burst activity across northern Australia in January and February (Cowan, Wheeler, Sharmila, Narsey, & de Burgh-Day, 2022) due to the reliability of the MJO. The correlation coefficient between detrended AUMR and the Niño 3.4 index (used to represent ENSO) is strongly significant ($R = -0.53$, $p < 0.001$; see Table 1). The stronger influence of equatorial Pacific SST anomalies (SSTa) on NE AUMR (e.g. Sharmila & Hendon, 2020) is reflected in the statistically significant correlations with all three Niño indices (Table 1), consistent with results acquired using the Southern Oscillation Index (SOI; Chung & Power, 2017). Based on the regression coefficients (β) obtained through MLR analysis (Table 1), AUMRV is mostly driven by ENSO (Niño 3.4). This finding is consistent with Zhu (2018) who found that the first Empirical Orthogonal Function (EOF) mode of all-Australian summer rainfall from 1960 to 2015 is linked to central Pacific SSTa and accounts for 30% of all-Australian summer rainfall variability, while the second EOF mode shows contrasting loadings over eastern and western Australia. Ocean–atmosphere interactions in the Indian Ocean enhance the impact of ENSO on the AUM (Taschetto et al., 2011; Wu & Kirtman, 2007), noting that the variability in the Indian Ocean is partly driven by ENSO (Zhong et al., 2005). SSTs in the Niño 3.4 region are also positively correlated with SSTs north of Australia between December and April, with the strongest correlation occurring in February (Catto et al., 2012). This contrasts with the presence of negative correlations between May and November.

Two types of El Niño events are distinguishable based on the zonal SSTa location in the equatorial Pacific (Ashok & Yamagata, 2009). These El Niño types have distinct impacts on AUMR (in DJFM) and Australia-wide rainfall in other seasons (e.g. Freund et al., 2021; Taschetto & England, 2009). We next review the impacts of these different ENSO event 'flavors' on AUMR. Monthly rainfall anomalies over NW and NE Australia during ENSO events are included in Figure 4 and the relationship between Eastern Pacific and Central Pacific indices by Ren and Jin (2011) and AUMR is shown in Figure 5.

3.1.1 | Eastern Pacific El Niño

During an Eastern Pacific (EP) El Niño event (see Heidemann et al., 2022 for definition using ENSO indices developed by Ren & Jin, 2011), the maximum SST warming is in the eastern equatorial Pacific (Rasmusson & Carpenter, 1982)
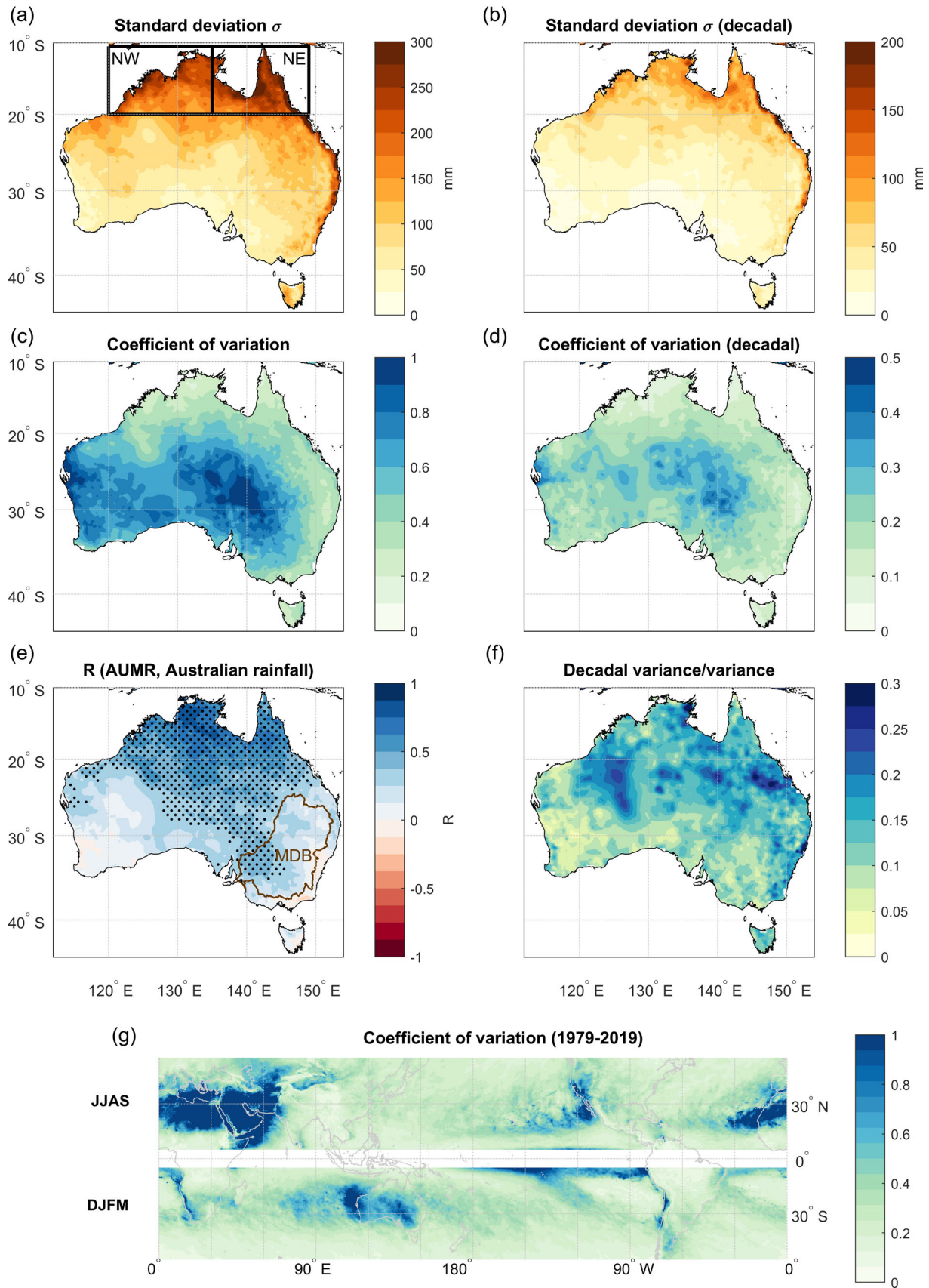
FIGURE 3   Legend on next page.

TABLE 1 Correlation coefficients (R) between detrended SST indices (for December to March [DJFM]: Niño 3.4, Niño 4, Niño 3, Tripole index [TPI], Indian Ocean Basin-wide warming [IOBW] index; and for September to November [SON]: Dipole mode index [DMI]) and detrended Australian monsoon rainfall (AUMR) anomalies over northern, northwest (NW) and northeast (NE) Australia, from 1920 to 2021

SST index	NW Australia		NE Australia		Northern Australia	
	R	β (MLR)	R	β (MLR)	R	β (MLR)
Niño 3.4	**−0.42**	−0.34	**−0.51**	−0.46	**−0.53**	−0.45
Niño 4	**−0.43**		**−0.53**		**−0.54**	
Niño 3	**−0.36**		**−0.44**		**−0.46**	
TPI	**−0.33**		**−0.50**		**−0.47**	
TPI (13-yr low-pass)	−0.04		−0.47		−0.28	
DMI (SON)	*−0.29*	−0.09	*−0.30*	−0.03	*−0.34*	−0.07
IOBW	**−0.35**	−0.05	**−0.42**	−0.06	**−0.44**	−0.06
		$R^2 = 0.18$		$R^2 = 0.26$		$R^2 = 0.28$

Notes: The indices are described in Appendix S1. R is noted as significant when $p < 0.05$ (italic R value) and highly significant as $p < 0.001$ (bold R value). Regression coefficients (β) are derived from multiple linear regression (MLR) analysis with AUMR as the response variable and the respective SST indices (Niño 3.4, DMI, IOBW) as predictors. The coefficient of determination (R^2) for the MLR analysis is included.

and lower tropospheric zonal winds over northern Australia in summer weaken (Kajikawa et al., 2010). Consequently, the first active monsoon phase or burst event is often delayed, leading to a below-average and shorter AUM season (Evans et al., 2014). During an EP El Niño's mature phase (October to March), northern Australia typically experiences below average rainfall (Freund et al., 2021), confirmed in this review using observations from 1920 to 2021 (not shown).

EP El Niño events drive rainfall deficits in the November to April wet season across NW (Figure 4a) and NE Australia (Figure 4b). The exception is January in the NW, when rainfall is close to climatology. Stronger amplitude El Niño events do not necessarily lead to a greater rainfall reduction, due to the nonlinear ENSO-AUMR relationship and an insignificant correlation between the SOI and summer rainfall over northern Australia during El Niño years (Chung & Power, 2017; Power et al., 2006). The correlations between EP El Niño events, represented by a positive EP index, and AUMR are weak and insignificant over northern Australia (Figure 5a, red circles). The large spread of precipitation anomalies associated with the positive EP index suggests that other factors are more influential on precipitation over northern Australia, for example, local SSTa, as observed in austral spring (Van Rensch et al., 2015, 2019). Nonlinearity in the relationship is linked to large-scale shifts in rainfall patterns, and a weak decrease in AUMR during El Niño events (Chung & Power, 2017). Furthermore, strong El Niño events do not necessarily translate to a later AUM onset (Lisonbee & Ribbe, 2021).

3.1.2 | Central Pacific El Niño

During a Central Pacific (CP) El Niño event, the maximum SSTa are located nearer to the Dateline (Ashok et al., 2007) and through their teleconnection with northern Australia, they can influence both the AUM onset timing and retreat (Taschetto et al., 2009). During January and February, enhanced rainfall is caused by anomalous diabatic heating in the central Pacific, which triggers an atmospheric Rossby wave through a Gill–Matsuno mechanism (Taschetto et al. 2010a). This mechanism is seasonally phase-locked and only occurs when the South Pacific Convergence Zone (SPCZ) strengthens in austral summer (Taschetto et al. 2010a). Subsequently, an anomalous cyclonic circulation is

FIGURE 3 Characterizing variability of detrended December to March (DJFM) rainfall over Australia between 1920 and 2021, (a,b) standard deviation of Australian monsoon season rainfall on (a) interannual and (b) decadal timescales. (c,d) Coefficient of variation on (c) interannual and (d) decadal timescales. (e) Correlation coefficient between AUMR and Australian rainfall in DJFM. Black stippling marks significance for $p < 0.001$. Brown contours indicate the location of the Murray-Darling Basin (MDB). (f) Ratio of decadal to interannual variance of DJFM rainfall. g) Coefficient of variation for rainfall in monsoon regions globally, from the ERA5 dataset (Hersbach et al., 2020) for the Northern Hemisphere (JJAS) and the Southern Hemisphere monsoon season (DJFM).
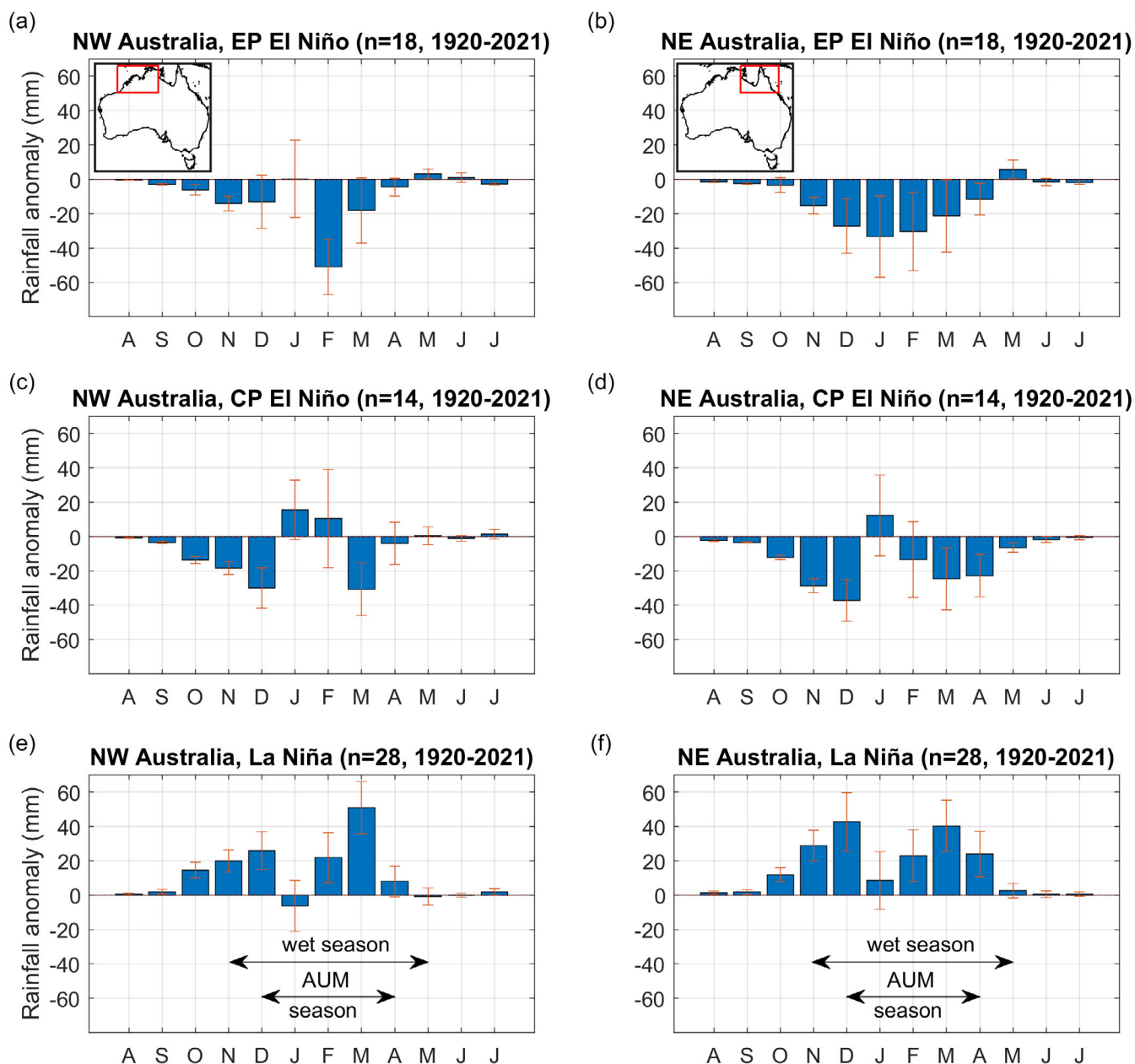
FIGURE 4 Composite annual cycle of spatially averaged northern Australian rainfall anomalies (northwest (NW) Australia: a,c,e; northeast (NE) Australia: b,d,f) during El Niño-Southern Oscillation (ENSO) events between 1920 and March 2021 using AWAP data. The time sequence begins in August of the developing ENSO event until July after the event termination. The anomalies are linearly detrended before the composite calculation. Error bars indicate the standard error ($\frac{\sigma}{\sqrt{n}}$) of the composite rainfall anomaly for each month.

formed off NW Australia, and the anomalous moisture convergence strengthens the mean monsoon circulation (Taschetto et al. 2010b). This leads to a reversal of the negative October–December rainfall anomalies to positive anomalies in January and February over NW Australia (Figure 4c). For NE Australia, rainfall is only weakly above average in January and below average for the remaining AUM months (Figure 4d).

3.1.3 | La Niña

Questions have been raised about whether CP and EP La Niña events (Ren & Jin, 2011) are distinguishable due to their similar SST patterns (Kug & Ham, 2011). Therefore, here we analyze the impact of La Niña events on AUMR as one single flavor, noting the well-established link between La Niña events and anomalously wet conditions over northern
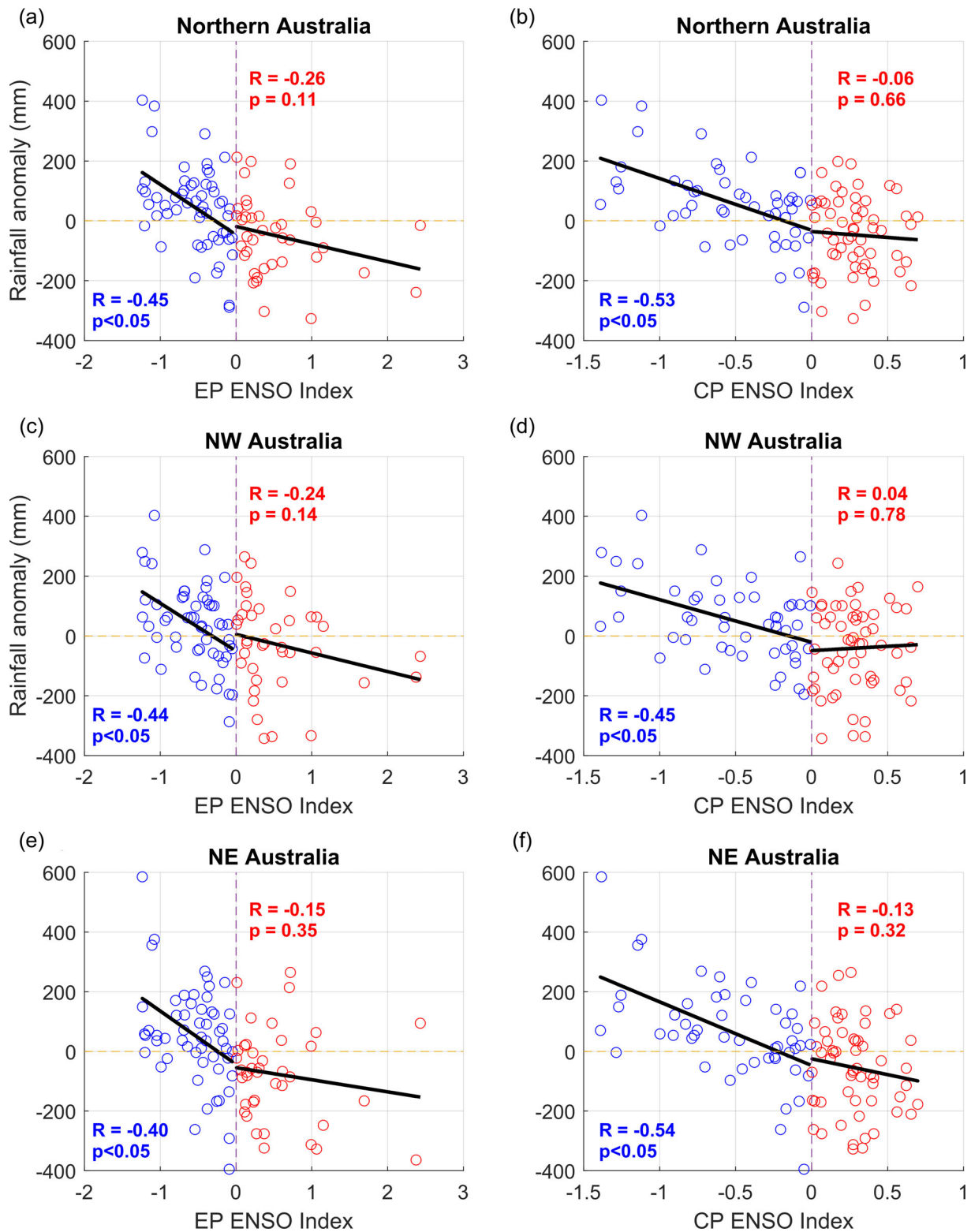
FIGURE 5 Relationship between December to March rainfall anomalies (mm) for northern Australia (a,b), NW Australia (c,d), and NE Australia (e,f) and the Ren and Jin (2011) ENSO Eastern Pacific (EP; a,c,e) and ENSO Central Pacific (CP; b,d,f) indices for the period 1920–2021 (blue circles: La Niña, red circles: El Niño). Both the rainfall and ENSO indices are linearly detrended.

Australia. In general, La Niña is associated with stronger zonal winds over northern Australia (Kajikawa et al., 2010), an earlier AUM onset (Evans et al., 2014), and above average AUMR (Wu & Kirtman, 2007). During strong La Niña events, the AUM tends to arrive about 14 days earlier than the climatological average (29 December), while for weak

La Niña events, the AUM onset is close to the climatology (Lisonbee & Ribbe, 2021). Except for January, where weak rainfall anomalies are observed, the composite rainfall over NE and NW Australia during La Niña events is well above average during the AUM season and shoulder months (Figure 4e,f).

While the SOI is significantly positively correlated with summer rainfall over northern Australia during La Niña events, stronger (weaker) La Niña events lead to larger (smaller) positive rainfall anomalies than a linear fit would imply (Chung & Power, 2017). The rainfall increase during La Niña can be attributed to a large-scale westward shift of anomalous rainfall over the equatorial Pacific (Chung & Power, 2017). We also find that AUMR over entire northern Australia, NE and NW Australia is significantly correlated to La Niña (Figure 5; blue circles). Warm SSTa north of Australia can supply additional moisture and enhance the impact of a La Niña event on NE Australia, as observed in 2010–2011 (Evans & Boyer-Souchet, 2012) when exceptionally high rainfall anomalies were recorded (Cai & Van Rensch, 2012). La Niña events are often associated with an anomalously wet austral autumn (Allen et al., 2020), and AUM-related rainfall bursts occur later in the wet season (i.e., April). This extends the AUM season (Cowan, Wheeler, Sharmila, Narsey, & de Burgh-Day, 2022).

3.2 | Indian Ocean climate modes and AUMR interannual variability

Wind-evaporation feedbacks in the Indian Ocean, the Indian Ocean Basin-wide Warming (IOBW), Ningaloo Niño and the Indian Ocean dipole (IOD) can also influence the AUM. We discuss their links with interannual AUMRV in further detail in the following section.

3.2.1 | Wind-evaporation feedbacks

Wind-evaporation feedbacks in the tropical south-eastern Indian Ocean (SEIO) are a dominant driver of interannual AUMRV over NW Australia. These feedbacks are a stronger cause for NW AUMRV than local or remote SSTa (Sekizawa et al., 2018). Enhanced westerly winds over the SEIO lead to a strengthening of the cyclonic circulation and monsoonal winds off NW Australia, which intensify evaporation and drive a further increase in NW rainfall during the wet season (Sharmila & Hendon, 2020). This rainfall-wind-evaporation feedback acts to maintain wet conditions for several years over NW Australia, making it an important mechanism for NW interannual AUMRV.

3.2.2 | Indian Ocean Basin-wide Warming

The impact of ENSO on the AUM can be reinforced by SST variability in the Indian Ocean. In coupled climate model targeted experiments, the influence of ENSO on the AUM is significantly reduced when the Indian Ocean is decoupled from the atmosphere (Wu & Kirtman, 2007). This is due to the IOBW mode (Chambers et al., 1999) that amplifies the impact of El Niño on AUMR (Taschetto et al., 2011). While El Niño induces IOBW through surface heat flux anomalies (Klein et al., 1999), the IOBW mode in turn feeds this signal back into the EP by dampening SSTs (Zhang et al., 2021). The forced response of the Indian Ocean to EP El Niño events enhances atmospheric subsidence and leads to a decrease in late summer rainfall over northern Australia (Taschetto et al., 2011). We find here that the IOBW mode and ENSO are highly correlated ($R = 0.76$, 1920–2021), consistent with a previous estimate ($R > 0.7$, 1949–2005; Taschetto et al., 2011). The strong ENSO-IOBW co-variability infers that the IOBW's impact on AUMR ($R = -0.44$) is due to ENSO, as confirmed from the MLR in Table 1 ($\beta = -0.06$). Subsequently, ocean–atmosphere interactions in the Indian Ocean play an important role in transmitting the ENSO signal across northern Australia.

3.2.3 | Ningaloo Niño

Ningaloo Niño events are characterized by warm SSTa and negative mean sea level pressure (MSLP) anomalies along Australia's west coast, which affect the large-scale atmospheric circulation and rainfall over Australia (Feng et al., 2013). The opposite applies to Ningaloo Niña events (Tozuka et al., 2014). Ningaloo Niño events peak in summer and are caused by wind-evaporation feedbacks in spring and anomalous poleward heat advection through the Leeuwin

current in summer. These events sometimes coincide with CP La Niña or even El Niño events (Marshall et al., 2015). Ningaloo Niño events can also amplify the strength of the trade winds during a La Niña event due to the anomalously low MSLP over the SEIO (Zhang & Han, 2018). Further, Ningaloo Niño events are linked to increased rainfall over western and northwestern Australia in January and February, associated with radiative heating and moisture advection (Zheng et al., 2020). Northern Australia can be affected in March and April (Marshall et al., 2015). In contrast, Ningaloo Niña events lead to decreased summer rainfall over NW Australia (Tozuka et al., 2014). To summarize, Ningaloo Niño (Niña) events have the potential to cause increased (decreased) rainfall especially over NW Australia.

3.2.4 | Indian Ocean dipole

The IOD is a prominent large-scale driver of Australia's climate, particularly in the southeast (Risbey et al., 2009), typically peaking in the austral spring. Being seasonally phase-locked (Saji et al., 1999), IOD events have a stronger impact on Australian spring rainfall and diminish before the AUM onset (Jourdain et al., 2013; Yoo et al., 2006). Given the strong ENSO-IOD relationship (Cai et al., 2011), when the co-varying ENSO signal is removed, the influence of the IOD on AUMR is negligible (Table 1). A positive IOD is defined when cool SSTa in the tropical SEIO and warm SSTa in the western Indian Ocean develop, encouraging anomalous easterly flow (Saji et al., 1999). Such easterlies to the north/northeast of Australia can occur from November to January (Chongyin & Mingquan, 2001), and can delay the AUM. Recent analysis suggests that there is a trend toward more positive IOD events since the mid-20th century (Abram et al., 2020), which has likely contributed to AUM onset delays in recent years (Lim et al., 2021; Lisonbee & Ribbe, 2021). In contrast, a negative IOD has a negligible impact on AUM onset timing (Lisonbee & Ribbe, 2021). Although the IOD has a weak impact on total AUMR, a positive IOD can influence the timing of the onset.

3.3 | Terrestrial processes and internal atmospheric variability

Terrestrial processes are considered important in influencing AUMRV, especially over NW Australia where the influence of ENSO is weak (Sharmila & Hendon, 2020). These processes are reviewed in the following section.

On a 5-year timescale, wet season rainfall variability is predominantly related to feedbacks between soil moisture and rainfall and a local rainfall-wind-evaporation feedback (Sharmila & Hendon, 2020). Higher soil moisture during anomalously wet years helps to drive increased evaporation over the NW in the following year, enhancing rainfall and sustaining the already wet conditions over multiple years (Sharmila & Hendon, 2020). The opposite is true for lower antecedent soil moisture conditions. Terrestrial variables such as the leaf area index and soil moisture anomalies account for about a third (36%) of the variance of northern Australian climate from January to March (Yu & Notaro, 2020). By climate, the authors are referring to convection, precipitation, total precipitable water, cloud cover, sea-level pressure and monsoon circulation over northern Australia. For comparison, oceanic influences explain 14% of the AUM variance in summer, which increases to 39% in autumn (1982–2015; Yu & Notaro, 2020). Therefore, oceanic influences and terrestrial feedbacks appear to be of similar importance for AUMV in late summer and autumn (Yu & Notaro, 2020).

In addition to tropical Indo-Pacific oceanic variability, atmospheric perturbations can also lead to extremely wet or dry conditions over Australia (Taschetto et al., 2016). By conducting coupled and atmosphere-only general circulation model experiments with a focus on east and west Australia, Taschetto et al. (2016) found that these wet or dry periods were less intense when oceanic variability was removed. Whether internal atmospheric processes are just as important for AUMR remains an open question.

In summary, interannual variability of AUMR is a clearly linked to ENSO, particularly over NE Australia. This has been confirmed across many studies (e.g., Evans et al., 2014; Forootan et al., 2016; Sharmila & Hendon, 2020; Wu & Kirtman, 2007). La Niña events are a major source for AUMR predictability due to their strong connection to early AUM onset and above average rainfall, while the relationship between El Niño and below average AUMR is weaker (Chung & Power, 2017). The strong teleconnection with ENSO makes NE Australia the region with most predictable AUMR. Over NW Australia, feedbacks involving local wind-evaporation and soil moisture play a more substantial role in summer rainfall (Sekizawa et al., 2018), and potentially maintain anomalous wet or dry conditions for consecutive years (Sharmila & Hendon, 2020). Variability in the Indian Ocean mostly influences AUMR through its co-variability

with ENSO (Taschetto et al., 2011). We find that interannual variability in AUMR and its associated drivers are well understood. In the next section, we delve into what influences decadal variations and multidecadal trends in AUMR.

4 | AUMR: DECADAL VARIABILITY, AND TRENDS

Statistics to characterize decadal AUMRV are shown in the right panels of Figure 3. Similar to interannual timescales, decadal variability is highest over northern Australia and near-coastal eastern Australia (Figure 3b). The standard deviation of decadal variability (σ_{decadal}) ranges from 14 mm in southwest Western Australia to over 100 mm near the eastern seaboard. Over the AUM region σ_{decadal} is 85 mm in the NW and 98 mm in the NE, leading to an average of 89 mm over the AUM region. The coefficient of (decadal) variation is 0.14 (Figure 3d).

The relative importance of decadal variability in rainfall to total variability has been previously investigated (Power, Tseitkin, Mehta, Lavery, Torok, & Holbrook, 1999). They found that decadal variability in annual precipitation was most influential over parts of northern Australia and next most influential over parts of central Australia and coastal New South Wales. We update this analysis and focus on the monsoon season. The resulting ratio ($\sigma^2_{\text{decadal}}/\sigma^2$; Figure 3f) shows that decadal variability accounts for the largest fraction of variability in central western Australia and in pockets of central Queensland. Over the AUM region, the ratio is slightly lower over the NW compared to the NE and overall averages to 0.17.

In the following subsections, we review links between decadal variability of SSTs and the AUM, with a specific focus on the Pacific Ocean (Section 4.1), other ocean basins (Section 4.2) and conclude in Section 4.3 with a discussion of multidecadal AUMR trends.

4.1 | Pacific Ocean decadal variability and AUMR

The Pacific Ocean exhibits a great deal of decadal variability, and much of this is linked to the Interdecadal Pacific Oscillation (IPO; Power et al., 2021). The relationship between Pacific decadal variability and AUMR is a topic of ongoing research and interest (e.g. Choi et al., 2016; Heidemann et al., 2022; Latif et al., 1997; Meehl & Arblaster, 2011). Decadal variability in northern Pacific SSTs is associated with the Pacific Decadal Oscillation (PDO; Jaffrés et al., 2018; Mantua & Hare, 2002), while the IPO is the larger-scale manifestation of decadal variability across the tropical and subtropical Indo-Pacific Oceans (Power, Casey, Folland, Colman, & Mehta, 1999). Both the IPO and PDO co-vary (e.g. Henley et al., 2015; Power, Casey, Folland, Colman, & Mehta, 1999) and are linked to the strength of the AUM circulation (Choi et al., 2016), variability in the AUM-ENSO teleconnection (Meehl & Arblaster, 2011) and decadal rainfall variations over NE Australia (Klingaman et al., 2013; Latif et al., 1997; Sharmila & Hendon, 2020). In fact, 22% of decadal variability in AUMR anomalies over NE Australia can be explained by the IPO, compared with 0.2% over the NW, based on a correlation between decadal variability (using a 13-year low-pass filter) in both the AUMR and the IPO Tripole index (TPI) (see Table 1).

The IPO is characterized by negative (nIPO) and positive (pIPO) phases, which are observed on a timescale from approximately 15–30 years (Folland et al., 2002; Power, Casey, Folland, Colman, & Mehta, 1999). The mean SSTa, as well as large-scale atmospheric conditions during nIPO and pIPO phases are shown in Figure 6, while AUMR anomalies are included in Figure 7. During nIPO phases, cool SSTa in the equatorial Pacific extend into the subtropical regions and are flanked by warmer SSTa to the north and south (Figure 6a). The opposite is true during pIPO phases (Figure 6b). Here we define the timeframes 1945–1976 and 1999–2014 as nIPO epochs, and 1924–1944 and 1977–1998 as pIPO epochs following Henley et al. (2015). The current IPO phase is unclear (Meehl et al., 2019), with more recent data indicating a potential return or continuation of a nIPO phase (Lim et al., 2021). In the following, we describe the relationship between pIPO and nIPO phases with AUMR as well as the decadal modulation of the ENSO-AUMR teleconnection.

During pIPO periods, warm SSTa extend towards the western tropical Pacific, shifting the major region of convection eastward and subsequently leading to subsidence and rainfall deficits over northern Australia (Arblaster et al., 2002) (Figure 7a). Both pIPO phases from 1924–1944 (Figure 7b) and 1977–1998 (Figure 7c) have resulted in AUMR deficits (Robertson et al., 2006), despite the weak relationship between AUMR and EP El Niño (and La Niña) events during these phases (Figure 8c,d) (Heidemann et al., 2022). To explain this, we show MSLP and 850 hPa wind anomalies averaged over the last two pIPO periods (Figure 6d), which indicate westerly anomalies in the central Pacific.
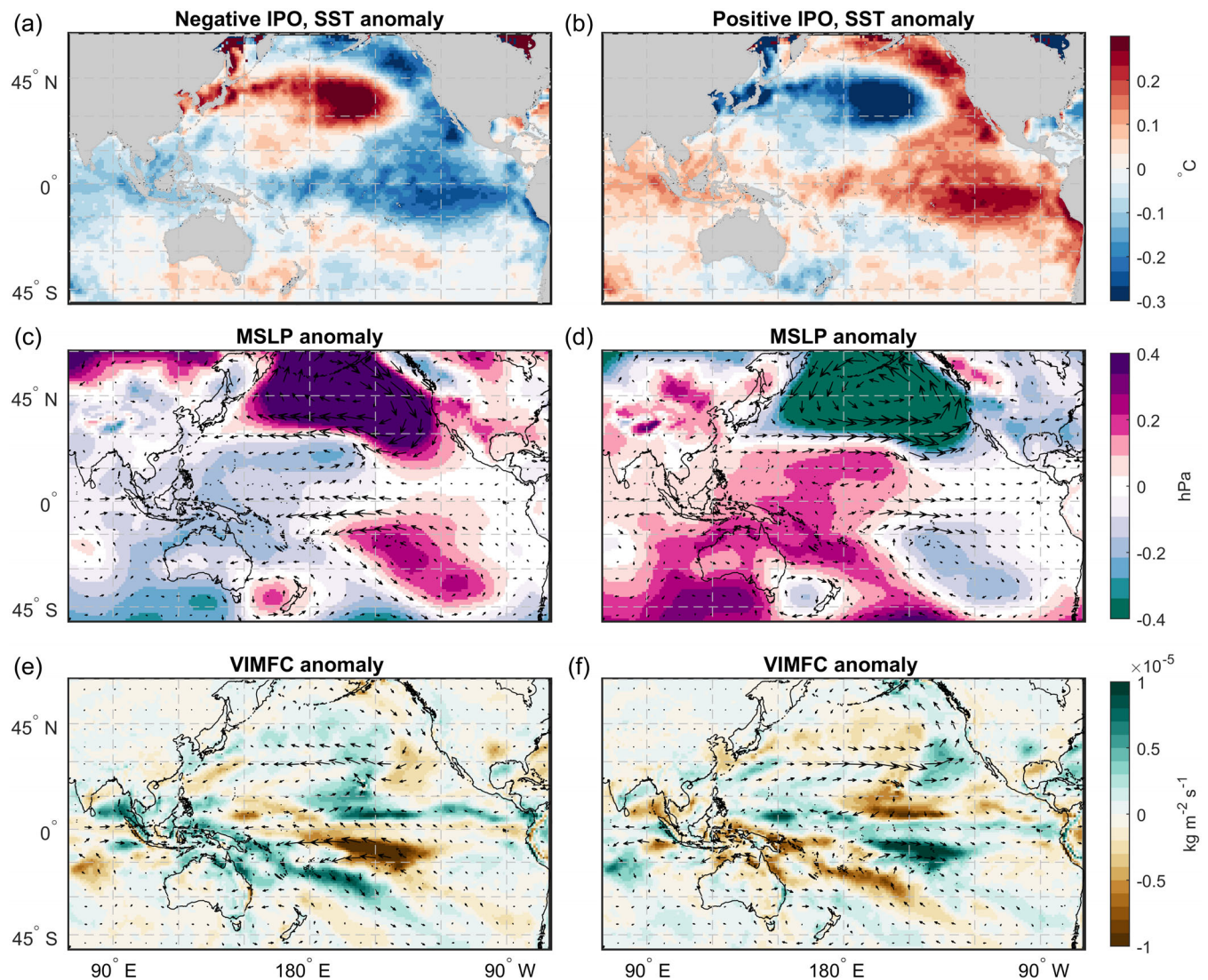
FIGURE 6 Sea surface temperature (SST) anomaly composites averaged over December to March during (a) negative (cool, 1945–1976 and 1999–2014) and (b) positive (warm, 1924–1944 and 1977–1998) Interdecadal Pacific Oscillation (IPO) phases; SST data were obtained from the Hadley Centre Global Sea ice and sea surface temperature (HadISST) v1.1 dataset (Rayner et al., 2003); MSLP (shading) and 850 hPa wind (vectors) anomalies during (c) negative and (d) positive IPO phases. Vertically integrated moisture flux convergence (VIMFC; shading) and integrated moisture flux (vectors) anomalies during (e) negative and (f) positive IPO phases. Monthly meridional and zonal winds, specific humidity and MSLP from the 20th century reanalysis version 3 dataset (Slivinski et al., 2019) were used for data shown in panels (c–f).

As such, the Walker Circulation shifts eastward and the easterly trade winds weaken, leading to decreased ocean–atmosphere coupling (Meehl & Arblaster, 2011). Anomalously high MSLP and anomalous divergence of moisture over the Maritime Continent and Australia (Figure 6d,f) support an eastward shift in convective activity, which even in La Niña conditions has little impact on Australia (Cai et al., 2010). Hence, northern Australia is disconnected from the tropical Pacific ENSO influence (Meehl & Arblaster, 2011) and the ENSO-AUMR teleconnection is weak (Arblaster et al., 2002), as shown during the most recent (1977–1998) pIPO phase (Suppiah, 2004; Yu & Janiga, 2007; Zhu, 2018).

As Figure 7d shows, decadal AUMR is above average during nIPO phases as it is over most of eastern Australia (Power, Casey, Folland, Colman, & Mehta, 1999). Positive rainfall anomalies are prominent over NE Australia in the nIPO epoch from 1945 to 1976. This is in contrast to the negative anomalies over the western half of the continent (Figure 7e) and consistent with Robertson et al. (2006). It is during the second nIPO epoch from 1999 to 2014 that positive anomalies spread to a wider area of northern Australia (Figure 7f).

During the two aforementioned nIPO phases, negative MSLP anomalies in the Indo-Australian region are accompanied by a weak cyclonic circulation over northern Australia, anomalous westerly winds in the western equatorial Indian Ocean and anomalous easterly winds in the central Pacific (Figure 6c). As a consequence, anomalous moisture
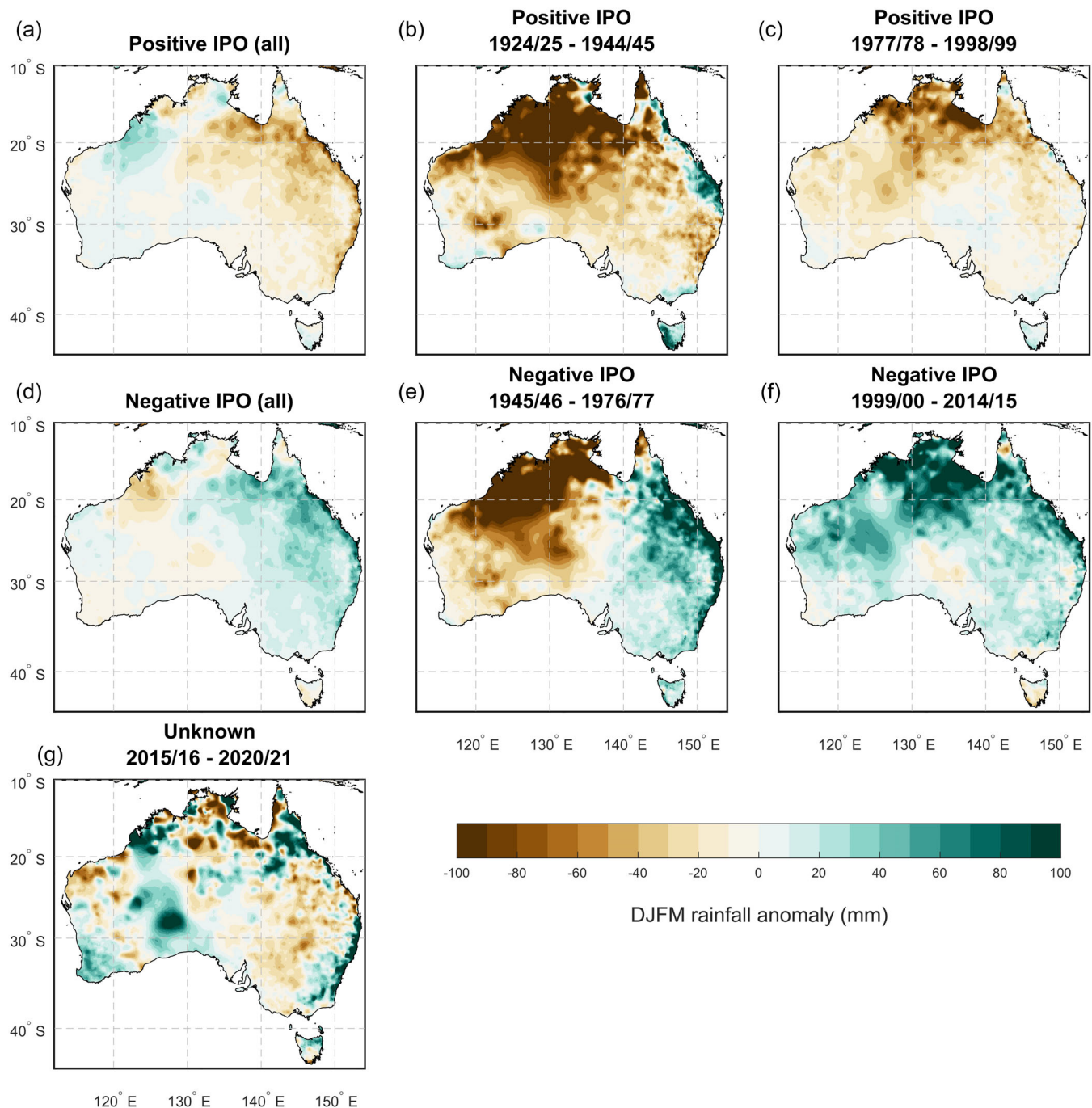
FIGURE 7 Observed Australian rainfall anomalies for December to March (DJFM) using AWAP data, averaged over the last two historic positive Interdecadal Pacific Oscillation (IPO) phases (a), and averaged over the last two historic negative IPO phases (d) using detrended data; for each individual IPO phase (b,c,e,f), and for the 2015–2021 period (g) in which the IPO phase is unclear.

flux convergence is observed over the Maritime Continent and over NE Australia along with a band of anomalous moisture convergence that stretches south-eastward into the South Pacific (Figure 6e). This reflects the following nIPO phase-specific features as found in previous studies: A westward shift and strengthening of the Pacific Walker Circulation (Meehl & Arblaster, 2011; Sharmila & Hendon, 2020) with its ascending branch located and convection center moving closer to northern Australia (Arblaster et al., 2002), a southwestward shift of the SPCZ (Folland et al., 2002) as well as a strengthening of the AUM circulation. The combination of all these factors favors rainfall especially over NE Australia during nIPO phases.
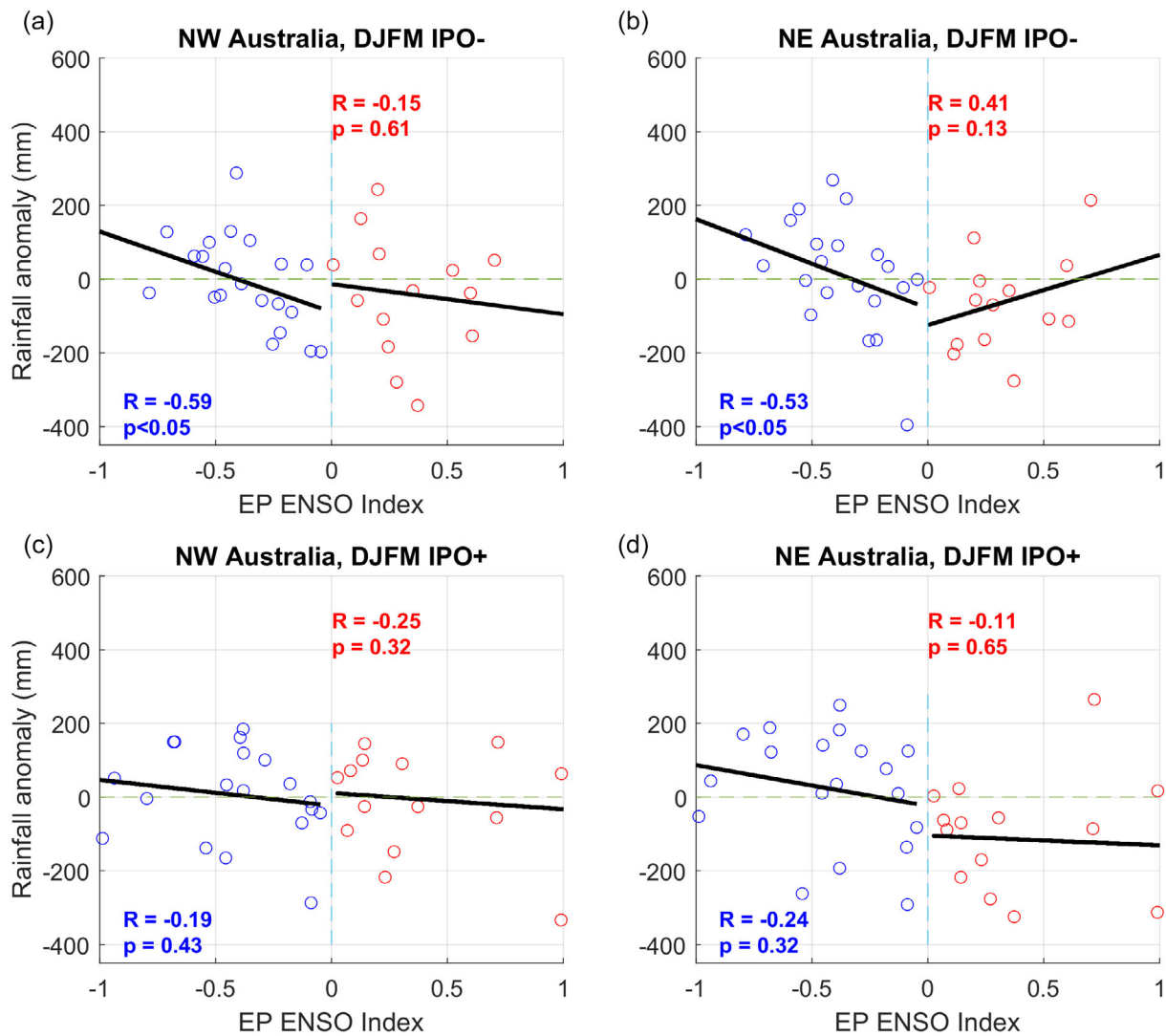
FIGURE 8 As in Figure 5, but separated into negative (a,b) and positive (c,d) Interdecadal Pacific Oscillation (IPO) phases for the Eastern Pacific (EP) index.

It is apparent that ENSO is more strongly connected to the AUM in nIPO phases compared to pIPO phases. This is because warm SSTa to the north and northeast of Australia are associated with the westward shift of the ascending branch of the Pacific Walker Circulation, which enables ENSO events to directly influence AUMR (Cai & Van Rensch, 2012). Cooler background SSTs in the tropical Pacific in nIPO phases are conducive for La Niña events to develop (Mantua & Hare, 2002). This more frequent occurrence of La Niña likely contributes to the reinforcement of the ENSO-AUMR teleconnection (Power & Colman, 2006), because La Niña events more strongly impact rainfall over northern (Chung & Power, 2017) and eastern Australia than El Niño events (King et al., 2013). The interannual intensification and southwest shift of the SPCZ during La Niña (Cai & Van Rensch, 2012), in combination with the nIPO influence on the SPCZ contributes to the anomalous NE rainfall response. Their combined effect leads to a further southwestward-located SPCZ compared to other combinations of IPO phases and ENSO events (Folland et al., 2002).

The increased likelihood of above average AUMR during La Niña within a nIPO phase is confirmed by the significantly strong negative correlations between AUMR and the negative CP (= Niño 4) and EP (= Niño 3) indices (Figures 8a,b and 9a,b). During La Niña events where cool SSTa peak in the central Pacific, a significantly positive AUMR response centered over NE Australia is recorded (Heidemann et al., 2022). CP El Niño events also impact AUMR more strongly during nIPO phases due to an anomalous anticyclone to the NW Australia and moisture flux divergence driving rainfall deficits (Heidemann et al., 2022).
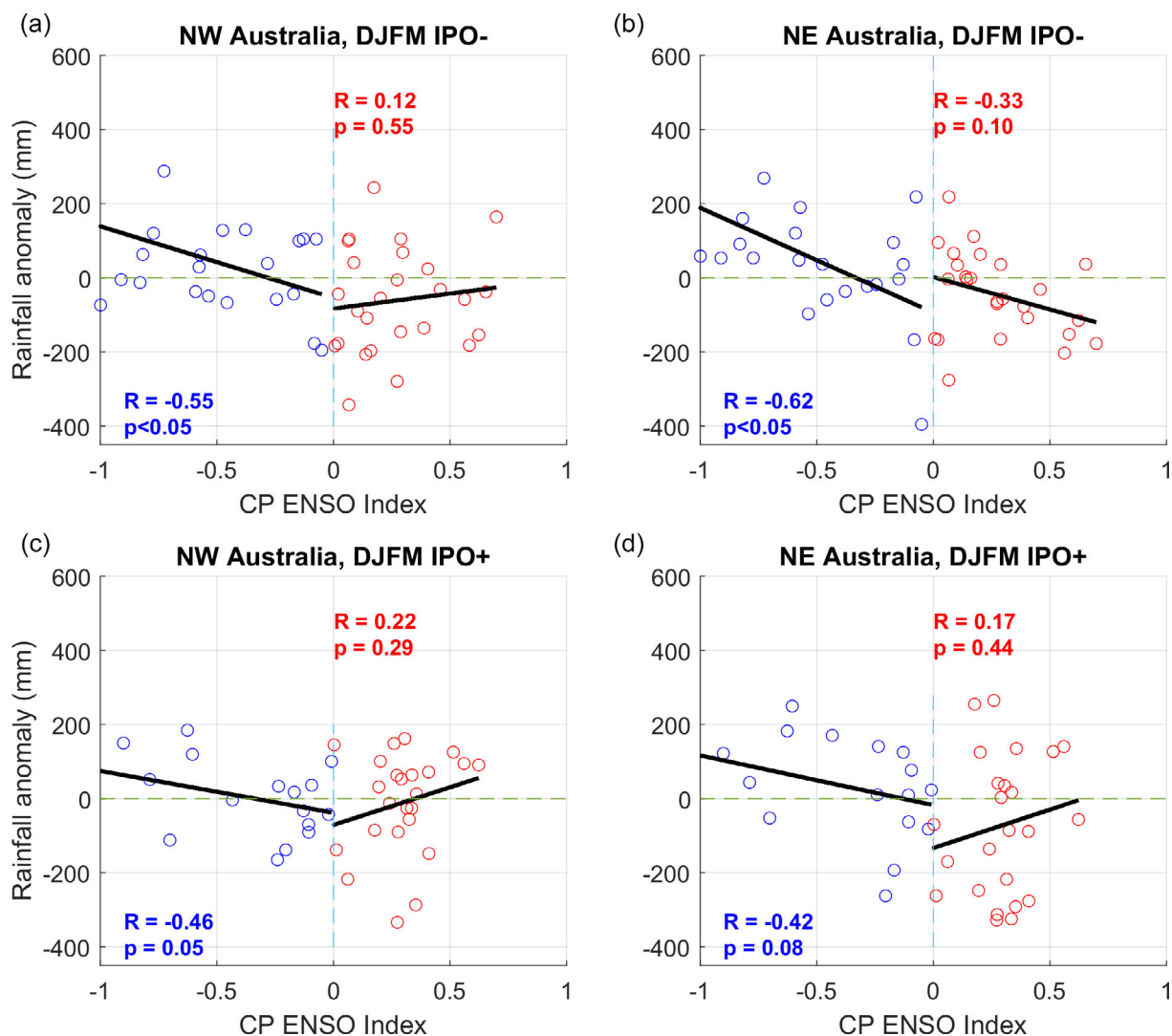
FIGURE 9 As in Figure 8, but for the Central Pacific (CP) index.

4.1.1 | Ningaloo Niño/Niña

Decadal variability of Ningaloo Niño/Niña events might be linked to AUMRV and the IPO. The connection of these events with western Australian summer to autumn (January to March) rainfall was relatively weak in the 1970–1990 period in contrast to the preceding and proceeding decades (Su et al., 2019). Ningaloo Niño events occur more frequently during nIPO phases due to warm SSTa off NW Australia and also exhibit a stronger local ocean–atmosphere coupling (Tanuma & Tozuka, 2020). This can lead to increased rainfall over NW Australia (Marshall et al., 2015). An nIPO-related increase in the frequency of Ningaloo Niño events might therefore contribute to decadally above-average rainfall over NW Australia during nIPO phases.

4.2 | Indian and Atlantic Ocean decadal variability and AUMR

Decadal SST variability in the Indian Ocean is much less explored than in the Pacific Ocean and has not explicitly been linked to AUMRV. It has been known for over two decades that the dominant EOF pattern of decadally (8-year low-pass) filtered Indian Ocean SST is in phase and significantly correlated with annual rainfall variability over eastern Australia (Power, Tseitkin, Mehta, Lavery, Torok, & Holbrook, 1999). Decadal variability of SSTs in the SEIO may indeed impact rainfall over NW Australia, in a similar manner to warm and cool Ningaloo Niño/ Niña events (i.e., via local

ocean–atmosphere interactions; Li, Han, Zhang, & Wang, 2019). Being negatively correlated with CP ENSO, the phases of the SEIO mode appear to respond to remote SST forcing in the central Pacific. A warm phase of the SEIO mode induces an anomalous cyclonic circulation in the southeast Indian Ocean, promoting above-average rainfall over NW Australia. This is not explicitly restricted to the AUM season though (Li, Han, Zhang, & Wang, 2019). The lack of research on the SEIO mode and its impact on regional rainfall should pave the way for future observational and modeling studies.

While the interannual influence of the IOBW on AUMR has been explored (Taschetto et al., 2011; see Section 3.2), any decadal modulation of this relationship due to the IPO remains uncertain. In pIPO phases, the correlation between Indian Ocean SST and AUMR is weak, as opposed to nIPO phases when the negative correlations are significant (Heidemann et al., 2022). IPO-related SST variability in the Indian Ocean and its impact on the Australian climate, also during ENSO events, is a topic that needs further attention.

The importance of the Atlantic Ocean for tropical climate variability and its teleconnection with other ocean basins is an emerging area of research (Cai et al., 2019). The warm Atlantic Multidecadal Oscillation (AMO) phase from 1932 to 1966 is hypothesized to have remotely impacted the atmospheric circulation over Australia (Nagaraju et al., 2018), when the influence of the Niño 3 SSTa and the IOBW on AUMR was weak despite the relatively strong AUM circulation (Ashok et al., 2014). Consequently, no significant negative rainfall anomalies were recorded over NE Australia during El Niño events (Ashok et al., 2014). The suggested mechanism for the warm AMO phase remotely influencing the AUM is as follows: warm SSTa over the extratropical north Atlantic are associated with increased vertical velocities (Nagaraju et al., 2018), which triggers a Rossby wave train that crosses the equator through the western Atlantic window. This is a region with mean upper tropospheric westerlies that allows a wave duct from the Northern to the Southern Hemisphere (Li, Feng, Li, & Hu 2019). The wave train is thought to induce upper-level divergence over northern Australia that strengthens the monsoonal westerlies and offsets the impact of El Niño events on AUMR (Nagaraju et al., 2018). However, these results are derived from only one warm AMO period, and it is speculative that the mechanism occurs across all warm AMO phases. Therefore, while the AMO could modify the impact El Niño imparts on the AUM circulation, further research is necessary to confirm this, especially as the influence of EP El Niño on AUMR is generally weak. We finally note that AMO variability is associated with variability in the IPO in one modeling study (Rashid et al., 2010) and this might provide a causal path by which Atlantic decadal variability could influence decadal AUMRV.

4.3 | Observed AUMR trends and proposed causality

Here, we expand on a review of all-Australian rainfall trends up to 2019 by Dey, Lewis, Arblaster, and Abram (2019) by including recent AUMR research. Rainfall over northern Australia during DJFM increased over the period 1920–2021 at a rate of 18 mm decade^{-1} (Figure 10a) and has accelerated to 24 mm decade^{-1} since 1950. The positive trend is generally weak over NE Australia (Figure 10c), but significantly strong over NW Australia (Figure 10b). In some parts of the northeast wet tropical climate zone, the trend is statistically significant, in contrast to long-term rainfall declines along the eastern Queensland coastal strip. The northern Australian rainfall increase has also been observed in the preceding months October and November (Freund et al., 2017). The multidecadal trend since the late 1970s (October to March) stands out particularly in comparison to previous multidecadal trends from proxy data reconstructions since 1600 (Freund et al., 2017). This highlights the sensitivity of trends and trend estimates to short observational records.

The question as to what is driving these long-term trends has generated numerous studies and hypotheses. One of those relates to the frequency of westerly wind bursts, that since the early 19th century have increased significantly (and accelerated since the 1950s) during mid-summer to the northwest of Australia (Gallego et al., 2017). Monsoon bursts lasting longer than 6 days have also become more frequent and prolonged over northern Australia since 1911 and shown the same acceleration since the 1950s (Dey et al., 2020). Another possible contribution to the increasing rainfall may be the more frequent occurrence of tropical cyclones and monsoon lows over NW Australia in the recent post-1980 decades. The increase in occurrence of synoptic systems that lead to heavy rainfall is responsible for the majority (70%) of the rainfall increase. Its cause needs to be further studied (Clark et al., 2018). A trend toward an earlier wet season onset has been recorded for the western and southwestern parts of northern Australia since the 1960s (Drosdowsky & Wheeler, 2014), consistent with a significant increase in early monsoon season burst days over the NW (Cowan, Wheeler, Sharmila, Narsey, & de Burgh-Day, 2022). Consistent with later retreat dates, the length of the wet season has significantly increased by +3.4 days decade^{-1}, meaning the wet season is 38.8 days longer in the present-
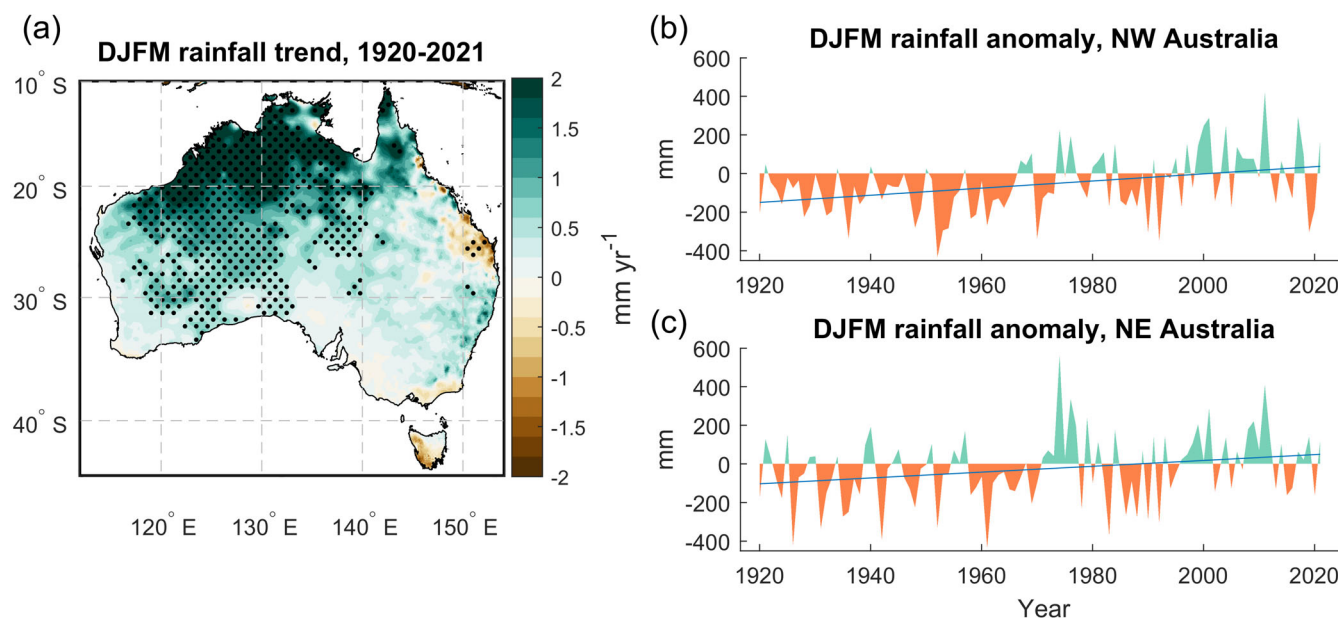
FIGURE 10 (a) Observed December to March (DJFM) rainfall trend between 1920 and 2021 using AWAP data; stippling indicates significance ($p < 0.05$) based on the nonparametric Mann–Kendall test. Timeseries of DJFM rainfall anomalies with respect to the 1981 to 2010 climatology for (b) NW Australia, and (c) NE Australia. The blue line indicates the linear trend.

day than in 1900 (Uehling & Misra, 2020). The increasing rainfall trend over NW Australia may partly be forced by anthropogenic aerosols (Rotstayn et al., 2012). Using aerosols-only simulations from CMIP5, Ha et al. (2020) find that anthropogenic aerosols over Asia induce a north–south thermal gradient that leads to southward cross-equatorial flow and a strengthening of the AUM. Dey, Lewis, and Abram (2019) suggest a strong role of aerosols as well, as the trend was not captured in CMIP5 historical greenhouse gas only (hist-GHG) and natural forcing only runs, but was better represented when all forcings where included. This also rules out the influence of greenhouse gases as a driver for the trend, which we can confirm for hist-GHG simulations in CMIP phase 6 (CMIP6), with 12 CMIP6 models capturing no significant trend in AUMR over NW Australia. Further process-based research is needed to confirm the role of aerosols in the increasing rainfall trend over the NW (Dey, Lewis, & Abram, 2019).

Another proposed contributing factor to the increasing rainfall trend over NW Australia is an SST warming trend in the tropical Atlantic Ocean. The warmer tropical SSTs help promote anomalous ascending air over the tropical Atlantic, which potentially triggers an anomalous atmospheric mid-latitude Rossby wave train in the southwestern Atlantic. The wave train travels eastward with the Southern Hemisphere westerly jet in austral summer and veers northeast toward Australia where the westerly jet exits. This induces upper-level divergence and wet conditions over NW Australia (Lin & Li, 2012). The wave train is therefore called the South Atlantic and South Indian Ocean pattern. It is associated with ascending motion and a negative surface temperature anomaly in the eastern Indian Ocean as well as convergence in the lower troposphere and strengthened westerly winds towards NW Australia (Lin, 2019). It has been suggested that the pattern may be caused by internal, interannual atmospheric variability that is related to zonal shifts of the South Atlantic Convergence Zone and is only weakly related to tropical Atlantic SSTs (Lin, 2019), highlighting the uncertainty about it. Further research is required to clarify the causes of the pattern, its associated variability, long-term changes and impacts on AUMR.

Finally, the tropical western Pacific may be connected to increasing rainfall over northern Australia. Since the early 1980s, there has been an acceleration in the SST amplitude and size of the Western Pacific Warm Pool, which may be responsible for slowing the movement of the MJO over the Maritime Continent when convectively active (in phases 5 to 7). This has led to an increase in the average duration of active MJO phases over the Maritime Continent by 5–6 days contributing to wetter conditions over northern Australia (Roxy et al., 2019).

In summary, our review of decadal variability and trends in AUMR finds that our knowledge on decadal variability and trends in AUMR is much more uncertain and speculative than for interannual AUMRV. One key driver of decadal AUMRV on which studies agree is the IPO (Klingaman et al., 2013; Latif et al., 1997; Sharmila & Hendon, 2020) and its influence on the ENSO-AUM teleconnection (Arblaster et al., 2002; Cai & Van Rensch, 2012; Heidemann et al., 2022; Meehl & Arblaster, 2011). Known key mechanisms for AUMRV due to the IPO generally include zonal shifts in the

Pacific Walker Circulation as well as its western rising branch (Meehl & Arblaster, 2011; Sharmila & Hendon, 2020) and the position of the SPCZ (Folland et al., 2002).

Unfortunately, this review finds that our knowledge regarding the influence of the Indian and Atlantic Ocean on decadal AUM variability is limited to two studies (Li, Han, Zhang, & Wang, 2019; Nagaraju et al., 2018). It further finds that due to the lack of consensus about the cause(s) of the increasing rainfall trend over NW Australia across the literature, this topic is yet to be resolved.

In the following section, we will focus on how the AUM is represented in coupled climate models from CMIP6 and how AUMR is projected to change in a warmer world.

5 | AUSTRALIAN MONSOON IN CLIMATE MODELS: HISTORICAL SIMULATIONS AND 21ST CENTURY PROJECTIONS

Compared to CMIP5, the CMIP6 modeling suite exhibits an improved representation of daily rainfall intensity over northern and eastern Australia (Grose et al., 2020). While the simulated mean December to May rainfall over northern Australia is also better in CMIP6 models, it is still underestimated (Grose et al., 2020) and this dry bias is strongest over NE Australia. Using the multimodel ensemble (MME) of 15 CMIP6 models, the correlation between the Oceanic Niño index and AUMR is slightly weaker than observed (Wang et al., 2020).

Future rainfall projections using the very high fossil fuel usage Shared Socioeconomic Pathway (SSP) 5–8.5 show a slight increase in precipitation over NE Australia for December to May by the end of the 21st century (2080–2099). However, there is low intermodel agreement over northern Australia (16 CMIP6 models; Grose et al., 2020). The spread of future projections for AUMR is lower in the CMIP6 MME than it is in the CMIP5 MME, though there is no consensus among the models on the sign of projected change, as 11 out of 23 CMIP6 models project an increase, 11 project a decrease, and one projects no change at all in summer rainfall over northern Australia. In models where Southern Hemisphere precipitation is projected to decrease (increase), AUMR is also projected to decrease (increase) by 2050–2099. This relationship has strengthened from CMIP5 to CMIP6 (Narsey et al., 2020).

As reported by Lee et al. (2021), the multimodel mean projection of 37 CMIP6 models indicates a statistically insignificant (less than 66% of model agree) increase in summer rainfall of up to 10% over northern Australia for the near future (2021–2040) under a scenario which implies high fossil fuel usage (SSP3-7.0; Lee et al., 2021). The same insignificant change and low intermodel agreement applies for the end of the 21st century (Lee et al., 2021). While in some isolated pockets within this broader region there appears to be a degree of agreement among models in each individual generation (i.e. CMIP3, CMIP5 and CMIP6) that the projected change is small (Grose et al., 2020; Power et al., 2012) and the locations of the pockets differ from one generation to the next. Subsequently, the confidence about future changes in AUMR is low (Douville et al., 2021).

6 | SUMMARY

This review provides an overview of the current state of knowledge about interannual and decadal Australian monsoon rainfall (AUMR) variability (AUMRV), how AUMR changed in the past and how AUMR might change in the future. A summary of the climate drivers affecting AUMRV as well as the potential causes for long-term changes is provided in Figure 11, which also depicts how strongly each driver influences AUMRV on interannual (upper panel) and decadal (second panel) timescales. Interactions between the drivers are also indicated. The most important findings are as follows:

1. Approximately 28% of interannual AUMRV is driven by oceanic processes ($R^2 = 0.28$, see Table 1) with the remaining variability linked to terrestrial feedbacks and internal atmospheric variability. The El Niño-Southern Oscillation (ENSO) is the dominant climate driver for interannual AUMRV (Chung & Power, 2017), reflecting, in part, the well-established relationship between La Niña and rainfall over northeast Australia. In contrast, AUMRV in northwest Australia is more strongly related to local terrestrial processes and wind-evaporation feedbacks (Sekizawa et al., 2018; Sharmila & Hendon, 2020). The impact of ENSO can be amplified or dampened by sea surface temperature anomalies to the north of Australia and in the Indian Ocean (Catto et al., 2012; Taschetto et al., 2011). Likewise, the Madden-Julian Oscillation also influences AUMRV (Cowan, Wheeler, & Marshall, 2023), making the accurate seasonal prediction of
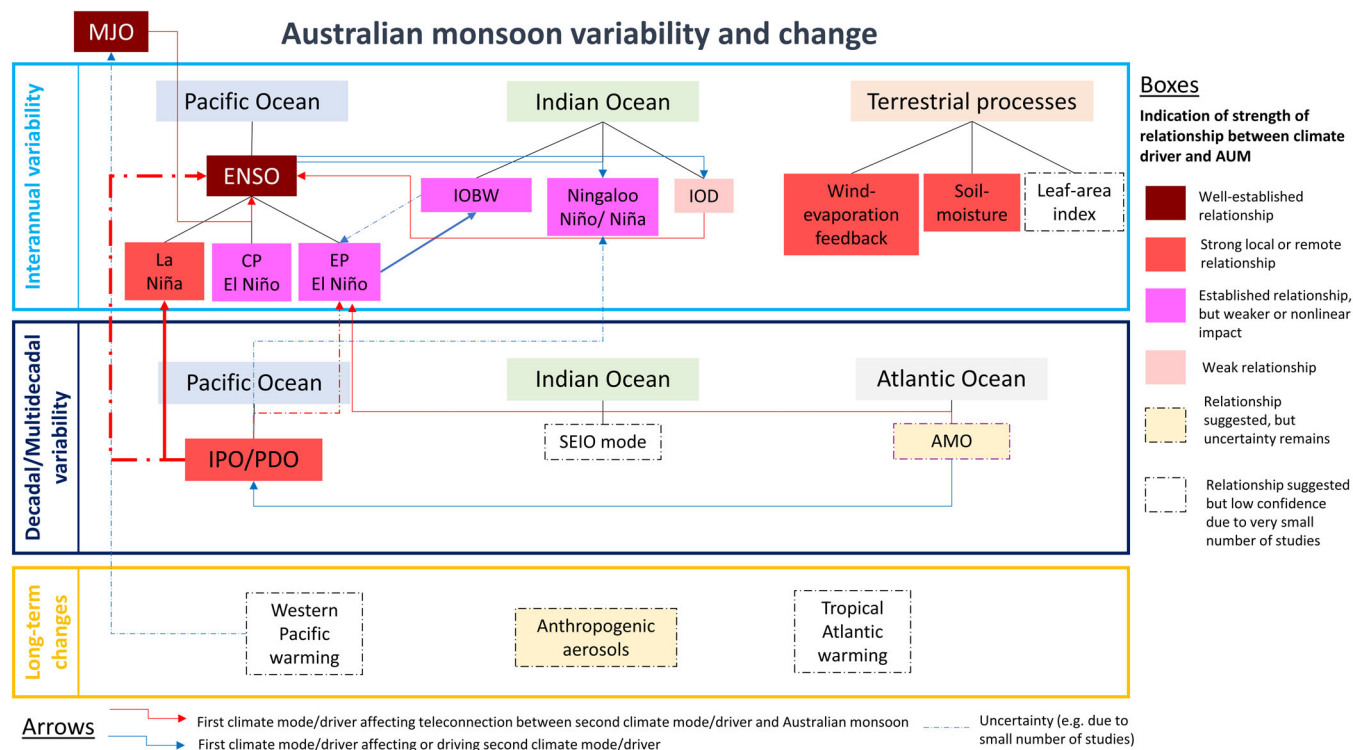
FIGURE 11 Summary of climate drivers affecting the Australian monsoon (AUM) on interannual to decadal timescales as well as the potential drivers for the recorded long-term changes in AUM rainfall. Small boxes represent local or remote climate drivers, which affect the AUM, divided into three timescales: Interannual variability is shown in the top panel, decadal to multidecadal variability in the middle panel, and long-term changes in the bottom panel. The color of each box indicates the strength of the relationship between the respective climate driver and the AUM, and also indicates uncertainty in the relationship with the AUM. The arrows show interconnections between several climate drivers across timescales: A blue arrow indicates that two climate drivers are connected; the climate driver at the beginning of the arrow affects or drives the climate driver at the end of the arrow (e.g. Eastern Pacific El Niño forces/modulates the IOBW). A red arrow indicates that the first climate driver (beginning of the arrow) impacts on the teleconnection between the AUM and the second climate driver (end of the arrow; e.g. the Interdecadal Pacific Oscillation, IPO, modifies the teleconnection between La Niña and the AUM). The thickness of the arrow indicates the strength of the modifications made to the relationship with the AUM (e.g. the IPO strongly affects the impact of La Niña on the AUM). A dashed arrow indicates uncertainty in an interconnection that might arise due to, for example, a small number of studies on a topic or results acquired through model experiments.

AUMR challenging. The strength of the relationship between AUMR and these climate drivers, including how they interact with each other, is indicated in the upper panel of Figure 11.

2. The AUMR exhibits strong decadal variability, which is primarily linked to the Interdecadal Pacific Oscillation (IPO). The phases of the IPO are associated with differences in the strength and zonal position of the Pacific Walker Circulation and the location of the South Pacific Convergence Zone (Folland et al., 2002; Meehl & Arblaster, 2011). Zonal shifts in maximum convergence across the Indo-Pacific are associated with decadal AUMR deficits (positive IPO phase) and increases (negative IPO phase) as well as a weakening (positive IPO) or strengthening (negative IPO) of the teleconnection between ENSO and AUMR.

3. In addition to decadal variability, a significant increasing trend in AUMR is evident, that is centered over northwest Australia. The increase of 18 mm decade^{-1} is equal to a 24% increase in AUMR from 1920 to 2021. Possible causing factors are: Western Pacific warming, anthropogenic aerosols and tropical Atlantic warming, as summarized in the third panel in Figure 11.

4. The representation of AUMR in coupled climate models has improved from CMIP5 to CMIP6. However, rainfall over northern Australia is still underestimated (Grose et al., 2020). Furthermore, near-term CMIP6 projections for the AUMR up to 2040 are uncertain (Lee et al., 2021). With a 50–50 split in CMIP6 models projecting an increase or decrease in AUMR by the end of the 21st century under high emissions scenarios, model agreement remains problematic (Narsey et al., 2020). Therefore, high uncertainty in relation to future AUMR projections exists due to little agreement on the sign of change over much of northern Australia.

7 | FUTURE RESEARCH PRIORITIES

While the mechanisms for interannual AUMRV are well-researched and understood, much less is known about decadal drivers of AUMRV and causes for its long-term trends.

In contrast to the established relationship between Pacific decadal variability and AUMRV, the decadal influence of the Atlantic and Indian Ocean on the AUM is highly uncertain. The role of Indian Ocean SSTs in transmitting the ENSO signal to the AUM region during different IPO phases warrants further investigation. For example, future research could explore differences in IOBW during El Niño events between positive and negative IPO phases. Likewise, the mechanisms that drive decadal AUMRV associated with CP El Niño events need further clarification. This can be explored through targeted climate model experiments, expanding on previous research (Taschetto et al. 2010a). This is because observational analyses of decadal variability are constrained by short observational data records, sparse observations, and limitations in data quality in the tropical Pacific prior to the 1960s (Power et al., 2021). It is recommended that additional attention is given to extending the coral proxy records further back in time, to be able to better study tropical variability and the modes of variability that drive it. This would also benefit investigations of the AUM by making longer records of decadal ENSO-related variability possible.

The cause of the trend in increasing rainfall over NW Australia during the observational period remains unclear, as highlighted by many studies suggesting different driving mechanisms for it. It is possible that the increasing trend in AUMR, which is strongest in the northwest (Dey, Lewis, Arblaster, & Abram, 2019), is linked to Indo-Pacific decadal variability and internal atmospheric variability. However, further research is needed to clarify the factors contributing to the trend and their relative importance.

With many climate drivers influencing AUMRV and change, future research should also focus on using a multivariate approach to see how the combination of climate drivers, across various time scales, alter the rainfall response over Australia (e.g. Lim et al., 2021). An example would be the combination of internal atmospheric and oceanic variability (e.g., ENSO event type and IOD event), which occur against background decadal variability and long-term mean-state changes. As explored in this review with a multiple linear regression approach on interannual timescales, we confirmed the dominant impact of ENSO on AUMR. Further exploration on the IOD's role in delaying or accelerating the AUM onset, and the associated atmospheric dynamics, is also warranted.

The underestimation of AUMRV in CMIP6 models reflects a broader issue in the representation of tropical precipitation. Hence, improving tropical convection and rainfall in coupled climate models is a high priority. This includes achieving a higher model spatial resolution to resolve local convective processes (Fiedler et al., 2020). The multiyear prediction and multidecadal projection of AUMR also remains an ongoing challenge. In addition, while progress has been made in understanding how ENSO and its teleconnections will change in the future (Cai et al., 2020; Power et al., 2021; Power & Delage, 2018) including ENSO teleconnections to Australia (Delage & Power, 2020), many uncertainties regarding the future variability and strength of ENSO events remain. ENSO and its interaction with the lower tropospheric circulation and rainfall anomalies in regions worldwide, including northern Australia, needs to be further studied.

A better understanding of processes that drive rainfall variability and change in the monsoonal northern Australia will—hopefully—lead to improved AUMR predictions and projections. This has the potential to contribute toward achieving a more sustainable future for agriculture and ecosystems in northern Australia.

AUTHOR CONTRIBUTIONS

Hanna Heidemann: Conceptualization (lead); formal analysis (lead); methodology (lead); resources (lead); visualization (lead); writing – original draft (lead); writing – review and editing (lead). **Tim Cowan:** Conceptualization (supporting); formal analysis (supporting); investigation (supporting); methodology (supporting); supervision (supporting); writing – original draft (supporting); writing – review and editing (supporting). **Benjamin J. Henley:** Methodology (supporting); supervision (supporting); writing – original draft (supporting). **Joachim Ribbe:** Supervision (supporting); writing – original draft (supporting); writing – review and editing (supporting). **Mandy Freund:** Methodology (supporting); writing – original draft (supporting). **Scott Power:** Methodology (supporting); supervision (supporting); writing – original draft (supporting); writing – review and editing (supporting).

resources and services from the National Computational Infrastructure (NCI), which is supported by the Australian Government. We would like to thank Emily Hinds and Chris Garth for providing us with the image of storm clouds near Darwin in northern Australia, which is shown in the graphical abstract. Open access publishing facilitated by University of Southern Queensland, as part of the Wiley - University of Southern Queensland agreement via the Council of Australian University Librarians.

CONFLICT OF INTEREST
The authors have declared no conflicts of interest for this article.

DATA AVAILABILITY STATEMENT
AWAP rainfall data are available upon request with the Australian Bureau of Meteorology. HadISST SST data are available on https://www.metoffice.gov.uk/hadobs/hadisst/data/download.html and provided by the UK MetOffice. 20CRv3 data can be acquired from https://psl.noaa.gov/data/gridded/data.20thC_ReanV3.html through NOAA. NCEP/NCAR data are available on NCEP/NCAR Reanalysis 1: NOAA Physical Sciences Laboratory through NOAA/ESRL/PSL. ERA5 data can be downloaded on the Climate Data Store https://cds.climate.copernicus.eu/.

ORCID
Hanna Heidemann https://orcid.org/0000-0003-0353-705X
Tim Cowan https://orcid.org/0000-0002-8376-4879
Benjamin J. Henley https://orcid.org/0000-0003-3940-1963
Joachim Ribbe https://orcid.org/0000-0001-6749-1228
Mandy Freund https://orcid.org/0000-0002-8839-5494
Scott Power https://orcid.org/0000-0002-9596-4368

RELATED WIREs ARTICLES
Review of tropical cyclones in the Australian region: Climatology, variability, predictability, and trends
A review of past and projected changes in Australia's rainfall

ENDNOTE
[1] See http://www.bom.gov.au/jsp/ncc/climate_averages/climate-classifications/index.jsp?maptype=kpngrp#maps

REFERENCES
Abram, N. J., Hargreaves, J. A., Wright, N. M., Thirumalai, K., Ummenhofer, C. C., & England, M. H. (2020). Palaeoclimate perspectives on the Indian Ocean dipole. *Quaternary Science Reviews*, *237*, 1–20. https://doi.org/10.1016/j.quascirev.2020.106302

Allen, K. J. J., Freund, M. B., Palmer, J. G., Simkin, R., Williams, L., Brookhouse, M., Cook, E. R., Stewart, S., & Baker, P. J. (2020). Hydroclimate extremes in a north Australian drought reconstruction asymmetrically linked with Central Pacific Sea surface temperatures. *Global and Planetary Change*, *195*, 1–11. https://doi.org/10.1016/j.gloplacha.2020.103329

Arblaster, J. M., Meehl, G. A., & Moore, A. M. (2002). Interdecadal modulation of Australian rainfall. *Climate Dynamics*, *18*, 519–531. https://doi.org/10.1007/s00382-001-0191-y

Ashok, K., Behera, S. K., Rao, S. A., Weng, H., & Yamagata, T. (2007). El Niño Modoki and its possible teleconnection. *Journal of Geophysical Research, Oceans*, *112*, 1–27. https://doi.org/10.1029/2006JC003798

Ashok, K., Nagaraju, C., Sen Gupta, A., & Pai, D. S. (2014). Decadal changes in the relationship between the Indian and Australian summer monsoons. *Climate Dynamics*, *42*, 1043–1052. https://doi.org/10.1007/s00382-012-1625-4

Ashok, K., & Yamagata, T. (2009). The El Niño with a difference. *Nature*, *461*, 481–484. https://doi.org/10.1038/461481a

Berry, G. J., & Reeder, M. J. (2016). The dynamics of Australian monsoon bursts. *Journal of the Atmospheric Sciences*, *73*, 55–69. https://doi.org/10.1175/JAS-D-15-0071.1

Bowman, D. M. J. S. (2002). The Australian summer monsoon: A biogeographic perspective. *Australian Geographical Studies*, *40*, 261–277. https://doi.org/10.1111/1467-8470.00179

Cai, W., Santoso, A., Wang, G., Wu, L., Collins, M., Lengaigne, M., Power, S., & Timmermann, A. (2020). ENSO response to greenhouse forcing. In M. J. McPhaden, A. Santoso, & W. Cai (Eds.), *El Niño southern oscillation in a changing climate Geophysical Monograph Series* (pp. 289–307). Wiley.

Cai, W., & Van Rensch, P. (2012). The 2011 Southeast Queensland extreme summer rainfall: A confirmation of a negative Pacific decadal oscillation phase? *Geophysical Research Letters*, *39*, 1–6. https://doi.org/10.1029/2011GL050820

Cai, W., Van Rensch, P., Cowan, T., & Sullivan, A. (2010). Asymmetry in ENSO teleconnection with regional rainfall, its multidecadal variability, and impact. *Journal of Climate*, *23*, 4944–4955. https://doi.org/10.1175/2010JCLI3501.1

Cai, W., Van Rensch, P., & Hendon, H. H. (2011). Teleconnection pathways of ENSO and the IOD and the mechanisms for impacts on Australian rainfall. *Journal of Climate*, *24*, 3910–3923. https://doi.org/10.1175/2011JCLI4129.1

Cai, W., Wu, L., Lengaigne, M., Li, T., Mcgregor, S., Kug, J. S., Yu, J. Y., Stuecker, M. F., Santoso, A., Li, X., Ham, Y. G., Chikamoto, Y., Ng, B., Mcphaden, M. J., Du, Y., Dommenget, D., Jia, F., Kajtar, J. B., Keenlyside, N., ... Chang, P. (2019). Pantropical climate interactions. *Science*, *363*, 1–11. https://doi.org/10.1126/science.aav4236

Catto, J. L., Nicholls, N., & Jakob, C. (2012). North Australian sea surface temperatures and the El Niño-Southern Oscillation in observations and models. *Journal of Climate*, *25*, 5011–5029. https://doi.org/10.1175/JCLI-D-11-00311.1

Chambers, D. P., Tapley, B. D., & Stewart, R. H. (1999). Anomalous warming in the Indian Ocean coincident with El Niño. *Journal of Geophysical Research, Oceans*, *104*, 3035–3047. https://doi.org/10.1029/1998jc900085

Chao, W. C., & Chen, B. (2001). The origin of monsoons. *Journal of the Atmospheric Sciences*, *58*, 3497–3507. https://doi.org/10.1175/1520-0469(2001)058<3497:TOOM>2.0.CO;2

Choi, K.-S., Kim, H.-D., & Kang, S.-D. (2016). Interdecadal variation of Australian summer monsoon during late 1990 s. *International Journal of Climatology*, *36*, 1917–1927. https://doi.org/10.1002/joc.4469

Chongyin, L., & Mingquan, M. (2001). The influence of the Indian Ocean dipole on atmospheric circulation and climate. *Advances in Atmospheric Sciences*, *18*, 830–843. https://doi.org/10.1007/BF03403506

Chung, C., & Power, S. B. (2017). The non-linear impact of El Niño, La Niña and the southern oscillation on seasonal and regional Australian precipitation. *Journal of Southern Hemisphere Earth Systems Science*, *67*, 25–45. https://doi.org/10.22499/3.6701.003

Clark, S., Reeder, M. J., & Jakob, C. (2018). Rainfall regimes over northwestern Australia. *Quarterly Journal of the Royal Meteorological Society*, *144*, 458–467. https://doi.org/10.1002/qj.3217

Cobon, D. H., Kouadio, L., Mushtaq, S., Jarvis, C., Carter, J., Stone, G., & Davis, P. (2019). Evaluating the shifts in rainfall and pasture-growth variabilities across the pastoral zone of Australia during 1910-2010. *Crop & Pasture Science*, *70*, 634–647. https://doi.org/10.1071/CP18482

Cowan, T., Wheeler, M., & Marshall, A. (2023). The combined influence of the Madden-Julian Oscillation and El Niño-Southern Oscillation on Australian rainfall. *Journal of Climate*, *36*, 313–334. https://doi.org/10.1175/JCLI-D-22-0357.1

Cowan, T., Wheeler, M. C., Sharmila, S., Narsey, S., & de Burgh-Day, C. (2022). Forecasting northern Australian summer rainfall bursts using a seasonal prediction system. *Weather and Forecasting*, *37*, 23–44. https://doi.org/10.1175/WAF-D-21-0046.1

Delage, F., & Power, S. B. (2020). The impact of global warming and the El Niño-southern oscillation on seasonal precipitation extremes in Australia. *Climate Dynamics*, *54*, 4367–4377. https://doi.org/10.1007/s00382-020-05235-0

Dey, R., Gallant, A. J. E., & Lewis, S. C. (2020). Evidence of a continent-wide shift of episodic rainfall in Australia. *Weather and Climate Extremes*, *29*, 1–15. https://doi.org/10.1016/j.wace.2020.100274

Dey, R., Lewis, S. C., & Abram, N. J. (2019). Investigating observed northwest Australian rainfall trends in coupled model Intercomparison project phase 5 detection and attribution experiments. *International Journal of Climatology*, *39*, 112–127. https://doi.org/10.1002/joc.5788

Dey, R., Lewis, S. C., Arblaster, J. M., & Abram, N. J. (2019). A review of past and projected changes in Australia's rainfall. *WIREs Climate Change*, *10*, 1–23. https://doi.org/10.1002/wcc.577

Douville, H., Raghavan, K., Renwick, J., Allan, R. P., Arias, A., Barlow, M., Cerezo-Mota, R., Cherchi, A., Gan, T. Y., Gergis, J., Jiang, D., Khan, A., Pokam Mba, W., Rosenfeld, D., Tierney, J., Zolina, O. (2021). Water cycle changes. In R. Yu, B. Zhou, V. Masson-Delmotte, P. Zhai, A. Pirani, S. L. Connors, C. Péan, S. Berger, N. Caud, Y. Chen, L. Goldfarb, M. I. Gomis, M. Huang, K. Leitzell, E. Lonnoy, J. B. R. Matthews, T. K. Maycock, T. Waterfield, & O. Yelekçi (Eds.), *Climate change 2021: The physical science basis. Contribution of working group I to the sixth assessment report of the intergovernmental panel on climate change* (pp. 1055–1210). Cambridge University Press.

Drosdowsky, W. (1996). Variability of the Australian summer monsoon at Darwin: 1957-1992. *Journal of Climate*, *9*, 85–96. https://doi.org/10.1175/1520-0442(1996)009<0085:VOTASM>2.0.CO;2

Drosdowsky, W., & Wheeler, M. C. (2014). Predicting the onset of the north Australian wet season with the POAMA dynamical prediction system. *Weather and Forecasting*, *29*, 150–161. https://doi.org/10.1175/WAF-D-13-00091.1

Evans, J. P., & Boyer-Souchet, I. (2012). Local sea surface temperatures add to extreme precipitation in Northeast Australia during La Niña. *Geophysical Research Letters*, *39*, 12–14. https://doi.org/10.1029/2012GL052014

Evans, S., Marchand, R., & Ackerman, T. (2014). Variability of the Australian monsoon and precipitation trends at Darwin. *Journal of Climate*, *27*, 8487–8500. https://doi.org/10.1175/JCLI-D-13-00422.1

Everingham, Y. L., Clarke, A. J., & Van Gorder, S. (2008). Long lead rainfall forecasts for the Australian sugar industry. *International Journal of Climatology*, *28*, 111–117. https://doi.org/10.1002/joc.1513

Feng, M., McPhaden, M. J., Xie, S. P., & Hafner, J. (2013). La Niña forces unprecedented Leeuwin current warming in 2011. *Scientific Reports*, *3*, 1–9. https://doi.org/10.1038/srep01277

Fiedler, S., Crueger, T., D'Agostino, R., Peters K., Becker, T., Leutwyler, D., Paccini L., Burdanowitz, J., Buehler, S. A., Uribe Cortes, A., Dauhut, T., Dommenget, D., Fraedrich, K., Jungandreas, L., Maher, N., Kristin Naumann, A., Rugenstein, M., Sakradzija, M., Schmidt, H., ... Stevens, B. (2020). Simulated tropical precipitation assessed across three major phases of the coupled model Intercomparison project (CMIP). *Monthly Weather Review*, *148*, 3653–3680. https://doi.org/10.1175/mwr-d-19-0404.1

Folland, C. K., Renwick, J. A., Salinger, M. J., & Mullan, A. B. (2002). Relative influences of the interdecadal Pacific oscillation and ENSO on the South Pacific convergence zone. *Geophysical Research Letters*, *29*, 21-1–21-24. https://doi.org/10.1029/2001GL014201

Forootan, E., Khandu, Awange, J. L., Schumacher, M., Anyah, R. O., van Dijk, A. I. J. M., & Kusche, J. (2016). Quantifying the impacts of ENSO and IOD on rain gauge and remotely sensed precipitation products over Australia. *Remote Sensing of Environment*, *172*, 50–66. https://doi.org/10.1016/j.rse.2015.10.027

Freund, M., Henley, B. J., Karoly, D. J., Allen, K. J., & Baker, P. J. (2017). Multi-century cool and warm season rainfall reconstructions for Australia's major climatic regions. *Climate of the Past Discussions*, *13*, 1751–1770. https://doi.org/10.5194/cp-2017-28

Freund, M. B., Marshall, A. G., Wheeler, M. C., & Brown, J. N. (2021). Central Pacific El Niño as a precursor to summer drought-breaking rainfall over southeastern Australia. *Geophysical Research Letters*, *48*, 1–9. https://doi.org/10.1029/2020gl091131

Gadgil, S. (2018). The monsoon system: Land–sea breeze or the ITCZ? *Journal of Earth System Science*, *127*, 1–29. https://doi.org/10.1007/s12040-017-0916-x

Gallego, D., García-Herrera, R., Peña-Ortiz, C., & Ribera, P. (2017). The steady enhancement of the Australian summer monsoon in the last 200 years. *Scientific Reports*, *7*, 1–7. https://doi.org/10.1038/s41598-017-16414-1

Ghelani, R. P. S., Oliver, E. C. J., Holbrook, N. J., Wheeler, M. C., & Klotzbach, P. J. (2017). Joint modulation of Intraseasonal rainfall in tropical Australia by the Madden-Julian oscillation and El Niño-southern oscillation. *Geophysical Research Letters*, *44*, 10754–10761. https://doi.org/10.1002/2017GL075452

Grose, M. R., Narsey, S., Delage, F. P., Dowdy, A. J., Bador, M., Boschat, G., Chung, C., Kajtar, J. B., Rauniyar, S., Freund, M. B., Lyu, K., Rashid, H., Zhang, X., Wales, S., Trenham, C., Holbrook, N. J., Cowan, T., Alexander, L., Arblaster, J. M., & Power, S. (2020). Insights from CMIP6 for Australia's future climate. *Earth's Future*, *8*, e2019EF001469. https://doi.org/10.1029/2019ef001469

Ha, K. J., Kim, B. H., Chung, E. S., Chan, J. C. L., & Chang, C. P. (2020). Major factors of global and regional monsoon rainfall changes: Natural versus anthropogenic forcing. *Environmental Research Letters*, *15*, 1–10. https://doi.org/10.1088/1748-9326/ab7767

Heidemann, H., Ribbe, J., Cowan, T., Henley, B. J., Pudmenzky, C., Stone, R., & Cobon, D. H. (2022). The influence of interannual and decadal Indo-Pacific Sea surface temperature variability on Australian monsoon rainfall. *Journal of Climate*, *35*, 425–444. https://doi.org/10.1175/JCLI-D-21-0264.1

Hendon, H. H., & Liebmann, B. (1990a). The intraseasonal 30-50 day oscillation of the Australian summer monsoon. *Journal of the Atmospheric Sciences*, *47*, 2909–2923. https://doi.org/10.1175/1520-0469(1990)047<2909:TIDOOT>2.0.CO;2

Hendon, H. H., & Liebmann, B. (1990b). A composite study of onset of the Australian summer monsoon. *Journal of the Atmospheric Sciences*, *47*, 2227–2240. https://doi.org/10.1175/1520-0469(1990)047<2227:acsooo>2.0.co;2

Hendon, H. H., Liebmann, B., Lim, E. P., & Liu, G. (2012). The role of air-sea interaction for prediction of Australian summer monsoon rainfall. *Journal of Climate*, *25*, 1278–1290. https://doi.org/10.1175/JCLI-D-11-00125.1

Henley, B. J., Gergis, J., Karoly, D. J., Power, S., Kennedy, J., & Folland, C. K. (2015). A tripole index for the interdecadal Pacific oscillation. *Climate Dynamics*, *45*, 3077–3090. https://doi.org/10.1007/s00382-015-2525-1

Hersbach, H., Bell, B., Berrisford, P., Hirahara, S., Horányi, A., Muñoz-Sabater, J., Nicolas, J., Peubey, C., Radu, R., Schepers, D., Simmons, A., Soci, C., Abdalla, S., Abellan, X., Balsamo, G., Bechtold, P., Biavati, G., Bidlot, J., Bonavita, M., ... Thépaut, J. N. (2020). The ERA5 global reanalysis. *Quarterly Journal of the Royal Meteorological Society*, *146*, 1999–2049. https://doi.org/10.1002/qj.3803

Holland, G. J. (1986). Interannual variability of the Australian summer monsoon at Darwin: 1952-82. *Monthly Weather Review*, *114*, 594–604. https://doi.org/10.1175/1520-0493(1986)114<0594:IVOTAS>2.0.CO;2

Hung, C.-W., & Yanai, M. (2004). Factors contributing to the onset of the Australian summer monsoon. *Quarterly Journal of the Royal Meteorological Society*, *130*, 739–758. https://doi.org/10.1256/qj.02.191

Jaffrés, J. B. D., Cuff, C., Rasmussen, C., & Hesson, A. S. (2018). Teleconnection of atmospheric and oceanic climate anomalies with Australian weather patterns: A review of data availability. *Earth-Science Reviews*, *176*, 117–146. https://doi.org/10.1016/j.earscirev.2017.08.010

Jones, D. A., Wang, W., & Fawcett, R. (2009). High-quality spatial climate data-sets for Australia. *Australian Meteorological and Oceanographic Journal*, *58*, 233–248. https://doi.org/10.22499/2.5804.003

Jourdain, N. C., Gupta, A. S., Taschetto, A. S., Ummenhofer, C. C., Moise, A. F., & Ashok, K. (2013). The Indo-Australian monsoon and its relationship to ENSO and IOD in reanalysis data and the CMIP3/CMIP5 simulations. *Climate Dynamics*, *41*, 3073–3102. https://doi.org/10.1007/s00382-013-1676-1

Kalnay, E., Kanamitsu, M., Kistler, R., Collins, W., Deaven, D., Gandin, L., Iredell, M., Saha, S., White, G., Woollen, J., Zhu, Y., Leetmaa, A., Reynolds, R., Chelliah, M., Ebisuzaki, W., Higgins, W., Janowiak, J., Mo, K. C., Ropelewski, C., ... Joseph, D. (1996). The NCEP/NCAR 40-year reanalysis project. *Bulletin of the American Meteorological Society*, *77*(3), 437–471. https://doi.org/10.1175/1520-0477(1996)077<0437:tnyrp>2.0.co;2

Kajikawa, Y., Wang, B., & Yang, J. (2010). A multi-time scale Australian monsoon index. *International Journal of Climatology*, *30*, 1114–1120. https://doi.org/10.1002/joc.1955

Kawamura, R., Fukuta, Y., Ueda, H., Matsuura, T., & Iizuka, S. (2002). A mechanism of the onset of the Australian summer monsoon. *Journal of Geophysical Research – Atmospheres*, *107*, ACL 5-1–ACL 5-15. https://doi.org/10.1029/2001JD001070

Kiladis, G. N., Wheeler, M. C., Haertel, P. T., Straub, K. H., & Roundy, P. E. (2009). Convectively coupled equatorial waves in reanalysis data. *Reviews of Geophysics*, *47*, 1–42. https://doi.org/10.1029/2008RG000266.1.HISTORICAL

King, A. D., Alexander, L. V., & Donat, M. G. (2013). Asymmetry in the response of eastern Australia extreme rainfall to low-frequency Pacific variability. *Geophysical Research Letters*, *40*, 2271–2277. https://doi.org/10.1002/grl.50427

Klein, S. A., Soden, B. J., & Lau, N. C. (1999). Remote Sea surface temperature variations during ENSO: Evidence for a tropical atmospheric bridge. *Journal of Climate*, *12*, 917–932. https://doi.org/10.1175/1520-0442(1999)012<0917:RSSTVD>2.0.CO;2

Klingaman, N. P., Woolnough, S. J., & Syktus, J. (2013). On the drivers of inter-annual and decadal rainfall variability in Queensland, Australia. *International Journal of Climatology*, *33*, 2413–2430. https://doi.org/10.1002/joc.3593

Kug, J. S., & Ham, Y. G. (2011). Are there two types of la Nina? *Geophysical Research Letters*, *38*, 2–7. https://doi.org/10.1029/2011GL048237

Latif, M., Kleeman, R., & Eckert, C. (1997). Greenhouse warming, decadal variability, or El Niño? An attempt to understand the anomalous 1990 s. *Journal of Climate*, *10*, 2221–2239. https://doi.org/10.1175/1520-0442(1997)010<2221:GWDVOE>2.0.CO;2

Lau, K.-M., & Yang, S. (2003). Walker Circulation. *Encyclopedia of Atmospheric Sciences*, 2505–2510. https://doi.org/10.1007/1-4020-3266-8_223

Lee, J. Y., Marotzke, J., Bala, G., Cao, L., Corti, S., Dunne, J. P., Engelbrecht, F., Fischer, E., Fyfe, J. C., Jones, C., Maycock, A., Mutemi, J., Ndiaye, O., Panickal, S., & Zhou, T. (2021). Future global climate: Scenario-based projections and near-term information. In R. Yu, B. Zhou, V. Masson-Delmotte, P. Zhai, A. Pirani, S. L. Connors, C. Péan, S. Berger, N. Caud, Y. Chen, L. Goldfarb, M. I. Gomis, M. Huang, K. Leitzell, E. Lonnoy, J. B. R. Matthews, T. K. Maycock, T. Waterfield, & O. Yelekçi (Eds.), *Climate change 2021: The physical science basis. Contribution of working group I to the sixth assessment report of the intergovernmental panel on climate change* (pp. 553–672). Cambridge University Press.

Li, Y., Feng, J., Li, J., & Hu, A. (2019). Equatorial windows and barriers for stationary Rossby wave propagation. *Journal of Climate*, *32*, 6117–6135. https://doi.org/10.1175/JCLI-D-18-0722.1

Li, Y., Han, W., Zhang, L., & Wang, F. (2019). Decadal SST variability in the southeast indian ocean and its impact on regional climate. *Journal of Climate*, *32*, 6299–6318. https://doi.org/10.1175/JCLI-D-19-0180.1

Lim, E.-P., Hudson, D., Wheeler, M. C., Marshall, A. G., King, A., Zhu, H., Hendon, H. H., de Burgh-Day, C., Trewin, B., Griffiths, M., Ramchurn, A., & Young, G. (2021). Why Australia was not wet during spring 2020 despite La Niña. *Scientific Reports*, *11*, 1–15. https://doi.org/10.1038/s41598-021-97690-w

Lin, Z. (2019). The South Atlantic-south Indian ocean pattern: A zonally oriented teleconnection along the southern hemisphere westerly jet in austral summer. *Atmosphere (Basel)*, *10*, 1–16. https://doi.org/10.3390/atmos10050259

Lin, Z., & Li, Y. (2012). Remote influence of the tropical Atlantic on the variability and trend in north West Australia summer rainfall. *Journal of Climate*, *25*, 2408–2420. https://doi.org/10.1175/JCLI-D-11-00020.1

Lisonbee, J., & Ribbe, J. (2021). Seasonal climate influences on the timing of the Australian monsoon onset. *Weather and Climate Dynamics*, *2*, 489–506. https://doi.org/10.5194/wcd-2-489-2021

Lisonbee, J., Ribbe, J., & Wheeler, M. (2020). Defining the north Australian monsoon onset: A systematic review. *Progress in Physical Geography*, *44*, 398–418. https://doi.org/10.1177/0309133319881107

Madden, R. A., & Julian, P. R. (1994). Observations of the 40-50-day tropical oscillation - A review. *Monthly Weather Review*, *122*, 814–837. https://doi.org/10.1175/1520-0493(1994)122<0814:OOTDTO>2.0.CO;2

Mantua, N. J., & Hare, S. R. (2002). The Pacific decadal oscillation. *Journal of Oceanography*, *58*, 35–44. https://doi.org/10.1023/A:1015820616384

Marshall, A. G., & Hendon, H. H. (2015). Subseasonal prediction of Australian summer monsoon anomalies. *Geophysical Research Letters*, *42*, 10913–10919. https://doi.org/10.1002/2015GL067086

Marshall, A. G., Hendon, H. H., Feng, M., & Schiller, A. (2015). Initiation and amplification of the Ningaloo Niño. *Climate Dynamics*, *45*, 2367–2385. https://doi.org/10.1007/s00382-015-2477-5

McKeon, G. A., Stone, G. A., Ahrens, D. A., Carter, J. B., Cobon, D. C., Irvine, S. A., & Syktus, J. A. (2021). Queensland' s multi-year wet and dry periods: Implications for grazing enterprises and pasture resources. *Rangeland Journal*, *43*, 121. https://doi.org/10.1071/RJ20089

Meehl, G. A., & Arblaster, J. M. (2011). Decadal variability of Asian-Australian monsoon-ENSO-TBO relationships. *Journal of Climate*, *24*, 4925–4940. https://doi.org/10.1175/2011JCLI4015.1

Meehl, G. A., Arblaster, J. M., Chung, C. T. Y., Holland, M. M., DuVivier, A., Thompson, L. A., Yang, D., & Bitz, C. M. (2019). Sustained ocean changes contributed to sudden Antarctic Sea ice retreat in late 2016. *Nature Communications*, *10*, 1–9. https://doi.org/10.1038/s41467-018-07865-9

Meinke, H., & Stone, R. C. (2005). Seasonal and inter-annual climate forecasting: The new tool for increasing preparedness to climate variability and change in agricultural planning and operations. In J. Salinger, M. V. K. Sivakumar, & R. P. Motha (Eds.), *Increasing climate variability and change: Reducing the vulnerability of agriculture and forestry* (pp. 221–253). Springer.

Moise, A., Smith, I., Brown, J. R., Colman, R., & Narsey, S. (2020). Observed and projected intra-seasonal variability of Australian monsoon rainfall. *International Journal of Climatology*, *40*, 2310–2327. https://doi.org/10.1002/joc.6334

Mollah, W. S., & Cook, I. M. (1996). Rainfall variability and agriculture in the semi-arid tropics - The Northern Territory, Australia. *Agricultural and Forest Meteorology*, *79*, 39–60. https://doi.org/10.1016/0168-1923(95)02267-8

Nagaraju, C., Ashok, K., Balakrishnan Nair, T. M., Guan, Z., & Cai, W. (2018). Potential influence of the Atlantic multi-decadal oscillation in modulating the biennial relationship between Indian and Australian summer monsoons. *International Journal of Climatology*, *38*, 5220–5230. https://doi.org/10.1002/joc.5722

Narsey, S. Y., Brown, J. R., Colman, R. A., Delage, F., Power, S. B., Moise, A. F., & Zhang, H. (2020). Climate change projections for the Australian monsoon from CMIP6 models. *Geophysical Research Letters*, *47*, 1–9. https://doi.org/10.1029/2019gl086816

Nicholls, N., McBride, J. L., & Ormerod, R. J. (1982). On predicting the onset of the Australian wet season at Darwin. *Monthly Weather Review*, *110*, 14–17. https://doi.org/10.1175/1520-0493(1982)110<0014:OPTOOT>2.0.CO;2

Nie, J., Boos, W. R., & Kuang, Z. (2010). Observational evaluation of a convective quasi-equilibrium view of monsoons. *Journal of Climate*, *23*, 4416–4428. https://doi.org/10.1175/2010JCLI3505.1

Pope, M., Jakob, C., & Reeder, M. J. (2009). Regimes of the north Australian wet season. *Journal of Climate*, *22*, 6699–6715. https://doi.org/10.1175/2009JCLI3057.1

Power, S., Casey, T., Folland, C., Colman, A., & Mehta, V. (1999). Inter-decadal modulation of the impact of ENSO on Australia. *Climate Dynamics*, *15*, 319–324. https://doi.org/10.1007/s003820050284

Power, S., & Colman, R. (2006). Multi-year predictability in a coupled general circulation model. *Climate Dynamics*, *26*, 247–272. https://doi.org/10.1007/s00382-005-0055-y

Power, S., Tseitkin, F., Mehta, V., Lavery, B., Torok, S., & Holbrook, N. (1999). Decadal climate variability in Australia during the twentieth century. *International Journal of Climatology*, *19*, 169–184. https://doi.org/10.1002/(SICI)1097-0088(199902)19:2<169::AID-JOC356>3.0.CO;2-Y

Power, S., Lengaigne, M., Capotondi, A., Khodri, M., Vialard, J., Jebri, B., Guilyardi, E., McGregor, S., Kug, J.-S., Newman, M., McPhaden, M. J., Meehl, G., Smith, D., Cole, J., Emile-Geay, J., Vimont, D., Wittenberg, A. T., Collins, M., Kim, G.-I., ... Henley, B. J. (2021). Decadal climate variability in the tropical Pacific: Characteristics, causes, predictability, and prospects. *Science*, *374*, 1–10. https://doi.org/10.1126/science.aay9165

Power, S. B., & Delage, F. (2018). El Niño-southern oscillation and associated climatic conditions around the world during the latter half of the twenty-first century. *Journal of Climate*, *31*, 6189–6207. https://doi.org/10.1175/JCLI-D-18-0138.1

Power, S. B., Delage, F., Colman, R., & Moise, A. (2012). Consensus on twenty-first-century rainfall projections in climate models more widespread than previously thought. *Journal of Climate*, *25*, 3792–3809. https://doi.org/10.1175/JCLI-D-11-00354.1

Power, S. B., Haylock, M., Colman, R., & Wang, X. (2006). The predictability of interdecadal changes in ENSO activity and ENSO teleconnections. *Journal of Climate*, *19*, 4755–4771. https://doi.org/10.1175/JCLI3868.1

Rashid, H. A., Power, S. B., & Knight, J. R. (2010). Impact of multidecadal fluctuations in the Atlantic thermohaline circulation on Indo-Pacific climate variability in a coupled GCM. *Journal of Climate*, *23*, 4038–4044. https://doi.org/10.1175/2010JCLI3430.1

Rasmusson, E. M., & Carpenter, T. H. (1982). Variations in tropical sea surface temperature and surface wind fields associated with the Southern Oscillation/El Niño. *Monthly Weather Review*, *110*, 354–384. https://doi.org/10.1175/1520-0493(1982)110<0354:VITSST>2.0.CO;2

Rayner, N. A., Parker, D. E., Horton, E. B., Folland, C. K., Alexander, L. V., Rowell, D. P., Kent, E. C., & Kaplan, A. (2003). Global analysis of sea surface temperature, sea ice, and night marine air temperature since the late nineteenth century. *Journal of Geophysical Research*, *108*, 1–56. https://doi.org/10.1029/2002JD002670

Ren, H. L., & Jin, F. F. (2011). Niño indices for two types of ENSO. *Geophysical Research Letters*, *38*, 1–5. https://doi.org/10.1029/2010GL046031

Risbey, J. S., Pook, M. J., McIntosh, P. C., Wheeler, M. C., & Hendon, H. (2009). On the remote drivers of rainfall variability in Australia. *Monthly Weather Review*, *137*, 3233–3253. https://doi.org/10.1175/2009mwr2861.1

Robertson, A. W., Kirshner, S., Smyth, P., Charles, S. P., & Bates, B. C. (2006). Subseasonal-to-interdecadal variability of the Australian monsoon over North Queensland. *Quarterly Journal of the Royal Meteorological Society*, *132*, 519–542. https://doi.org/10.1256/qj.05.75

Rotstayn, L. D., Jeffrey, S. J., Collier, M. A., Dravitzki, S. M., Hirst, A. C., Syktus, J. I., & Wong, K. K. (2012). Aerosol- and greenhouse gas-induced changes in summer rainfall and circulation in the Australasian region: A study using single-forcing climate simulations. *Atmospheric Chemistry and Physics*, *12*, 6377–6404. https://doi.org/10.5194/acp-12-6377-2012

Roxy, M. K., Dasgupta, P., Mcphaden, M. J., Suematsu, T., Zhang, C., & Kim, D. (2019). Twofold expansion of the Indo-Pacific warm pool warps the MJO life cycle. *Nature*, *575*, 647–651. https://doi.org/10.1038/s41586-019-1764-4

Saji, N. H., Goswami, B. N., Vinayachandran, P. N., & Yamagata, T. (1999). A dipole mode in the tropical Indian ocean. *Nature*, *401*, 360–363. https://doi.org/10.1038/43854

Sekizawa, S., Nakamura, H., & Kosaka, Y. (2018). Interannual variability of the Australian summer monsoon system internally sustained through wind-evaporation feedback. *Geophysical Research Letters*, *45*, 7748–7755. https://doi.org/10.1029/2018GL078536

Sharmila, S., & Hendon, H. H. (2020). Mechanisms of multiyear variations of Northern Australia wet-season rainfall. *Scientific Reports*, *10*, 1–11. https://doi.org/10.1038/s41598-020-61482-5

Slivinski, L. C., Compo, G. P., Whitaker, J. S., Sardeshmukh, P. D., Giese, B. S., McColl, C., Allan, R., Yin, X., Vose, R., Titchner, H., Kennedy, J., Spencer, L. J., Ashcroft, L., Brönnimann, S., Brunet, M., Camuffo, D., Cornes, R., Cram, T. A., Crouthamel, R., ... Wyszyński, P. (2019). Towards a more reliable historical reanalysis: Improvements for version 3 of the twentieth century reanalysis system. *Quarterly Journal of the Royal Meteorological Society*, *145*, 2876–2908. https://doi.org/10.1002/qj.3598

Su, L., Du, Y., Feng, M., & Li, J. (2019). Ningaloo Niño/Niña and their regional climate impacts as recorded by corals along the coast of Western Australia. *Palaeogeography, Palaeoclimatology, Palaeoecology*, *535*, 109368. https://doi.org/10.1016/j.palaeo.2019.109368

Sullivan, A., Zhong, W., Borzelli, G. L. E., Geng, T., Mackallah, C., Ng, B., Hong, C.-C., Cai, W., Huang, A. Y., & Bodman, R. (2021). Generation of westerly wind bursts by forcing outside the tropics. *Scientific Reports*, *11*, 1–12. https://doi.org/10.1038/s41598-020-79655-7

Suppiah, R. (1992). The Australian summer monsoon: A review. *Progress in Physical Geography*, *16*, 283–318. https://doi.org/10.1177/030913339201600302

Suppiah, R. (2004). Trends in the southern oscillation phenomenon and Australian rainfall and changes in their relationships. *International Journal of Climatology*, *24*, 269–290. https://doi.org/10.1002/joc.1001

Tanuma, N., & Tozuka, T. (2020). Influences of the interdecadal Pacific oscillation on the locally amplified Ningaloo Niño. *Geophysical Research Letters*, *47*, 1–8. https://doi.org/10.1029/2020GL088712

Taschetto, A. S., & England, M. H. (2009). El Niño Modoki impacts on Australian rainfall. *Journal of Climate*, *22*, 3167–3174. https://doi.org/10.1175/2008JCLI2589.1

Taschetto, A. S., Gupta, A. S., Hendon, H. H., Ummenhofer, C. C., & England, M. H. (2011). The contribution of Indian Ocean sea surface temperature anomalies on Australian summer rainfall during El Niño events. *Journal of Climate*, *24*, 3734–3747. https://doi.org/10.1175/2011JCLI3885.1

Taschetto, A. S., Haarsma, R. J., Gupta, A. S., Ummenhofer, C. C., Hill, K. J., & England, M. H. (2010a). Australian monsoon variability driven by a Gill-Matsuno-type response to central West Pacific warming. *Journal of Climate*, *23*, 4717–4736. https://doi.org/10.1175/2010JCLI3474.1

Taschetto, A. S., Haarsma, R. J., Sen Gupta, A., Ummenhofer, C. C., & England, M. H. (2010b). Teleconnections associated with the intensification of the Australian monsoon during El Niño Modoki events. *IOP Conference Series: Earth and Environmental Science*, *11*, 012031. https://doi.org/10.1088/1755-1315/11/1/012031

Taschetto, A. S., Sen Gupta, A., Jourdain, N. C., Santoso, A., Ummenhofer, C. C., & England, M. H. (2014). Cold tongue and warm pool ENSO events in CMIP5: Mean state and future projections. *Journal of Climate*, *27*, 2861–2885. https://doi.org/10.1175/JCLI-D-13-00437.1

Taschetto, A. S., Sen Gupta, A., Ummenhofer, C. C., & England, M. H. (2016). Can Australian multiyear droughts and wet spells be generated in the absence of oceanic variability? *Journal of Climate*, *29*, 6201–6221. https://doi.org/10.1175/JCLI-D-15-0694.1

Taschetto, A. S., Ummenhofer, C. C., Gupta, A. S., & England, M. H. (2009). Effect of anomalous warming in the Central Pacific on the Australian monsoon. *Geophysical Research Letters*, *36*, 1–5. https://doi.org/10.1029/2009GL038416

Tozuka, T., Kataoka, T., & Yamagata, T. (2014). Locally and remotely forced atmospheric circulation anomalies of Ningaloo Niño/Niña. *Climate Dynamics*, *43*, 2197–2205. https://doi.org/10.1007/s00382-013-2044-x

Troup, A. J. (1961). Variations in the upper tropospheric flow associated with the onset of the Australian summer monsoon. *Indian Journal of Meteorology & Geophysics*, *12*, 217–230. https://doi.org/10.54302/mausam.v12i2.4184

Uehling, J., & Misra, V. (2020). Characterizing the seasonal cycle of the northern australian rainy season. *Journal of Climate*, *33*, 8957–8973. https://doi.org/10.1175/JCLI-D-19-0592.1

Van Rensch, P., Arblaster, J., Gallant, A. J. E., Cai, W., Nicholls, N., & Durack, P. J. (2019). Mechanisms causing east Australian spring rainfall differences between three strong El Niño events. *Climate Dynamics*, *53*, 3641–3659. https://doi.org/10.1007/s00382-019-04732-1

Van Rensch, P., Gallant, A. J. E., Cai, W., & Nicholls, N. (2015). Evidence of local sea surface temperatures overriding the southeast Australian rainfall response to the 1997-1998 El Niño. *Geophysical Research Letters*, *42*, 9449–9456. https://doi.org/10.1002/2015GL066319

Wang, B., Jin, C., & Liu, J. (2020). Understanding future change of global monsoons projected by CMIP6 models. *Journal of Climate*, *33*, 6471–6489. https://doi.org/10.1175/JCLI-D-19-0993.1

Wang, B., Kang, I.-S., & Lee, J.-Y. (2004). Ensemble simulations of Asian-Australian monsoon variability by 11 AGCMs. *Journal of Climate*, *17*, 803–818. https://doi.org/10.1175/1520-0442(2004)017<0803:ESOAMV>2.0.CO;2

Wang, B., Biasutti, M., Byrne, M. P., Castro, C., Chang, C.-P., Cook, K., Fu, R., Grimm, A. M., Ha, K.-J., Hendon, H., Kitoh, A., Krishnan, R., Lee, J.-Y., Li, J., Liu, J., Moise, A., Pascale, S., Roxy, M. K., Seth, … Zhou, T. (2021). Monsoons climate change assessment. *Bulletin of the American Meteorological Society*, *102*, E1–E19. https://doi.org/10.1175/BAMS-D-19-0335.1

Webster, P. J., Magaña, V. O., Palmer, T. N., Shukla, J., Tomas, R. A., Yanai, M., & Yasunari, T. (1998). Monsoons: Processes, predictability, and the prospects for prediction. *Journal of Geophysical Research, Oceans*, *103*, 14451–14510. https://doi.org/10.1029/97jc02719

Wheeler, M. C., & Hendon, H. H. (2004). An all-season real-time multivariate MJO index: Development of an index for monitoring and prediction. *Monthly Weather Review*, *132*(8), 1917–1932. https://doi.org/10.1175/1520-0493(2004)132<1917:aarmmi>2.0.co;2

Wheeler, M. C., & McBride, J. (2007). Australian-Indonesian monsoon. In W. K. M. Lau & D. E. Waliser (Eds.), *Intraseasonal variability in the Atmosphere-Ocean climate system* (pp. 125–173). Springer.

Wheeler, M. C., & McBride, J. L. (2011). Australasian monsoon. In W. K. M. Lau & D. E. Waliser (Eds.), *Intraseasonal Variability in the Atmosphere-Ocean climate system* (2nd ed., pp. 147–194). Springer.

Wu, R., & Kirtman, B. P. (2007). Roles of the Indian Ocean in the Australian summer monsoon-ENSO relationship. *Journal of Climate*, *20*, 4768–4788. https://doi.org/10.1175/JCLI4281.1

Yoo, S.-H., Yang, S., & Ho, C.-H. (2006). Variability of the Indian Ocean sea surface temperature and its impacts on Asian-Australian monsoon climate. *Journal of Geophysical Research*, *111*(3), 1–1. https://doi.org/10.1029/2005jd006001

Yu, J.-Y., & Janiga, M. A. (2007). Changes in the in-phase relationship between the Indian and subsequent Australian summer monsoons during the past five decades. *Annales de Geophysique*, *25*, 1929–1933. https://doi.org/10.5194/angeo-25-1929-2007

Yu, Y., & Notaro, M. (2020). Observed land surface feedbacks on the Australian monsoon system. *Climate Dynamics*, *54*, 3021–3040. https://doi.org/10.1007/s00382-020-05154-0

Zhang, H., & Moise, A. (2016). The Australian summer monsoon in current and future climate. In L. M. V. de Carvalho & C. Jones (Eds.), *The monsoons and climate change* (pp. 67–120). Springer.

Zhang, L., & Han, W. (2018). Impact of Ningaloo Niño on tropical Pacific and an Interbasin coupling mechanism. *Geophysical Research Letters*, *45*, 11300–11309. https://doi.org/10.1029/2018GL078579

Zhang, L., Wang, G., Newman, M., & Han, W. (2021). Interannual to decadal variability of tropical indian ocean sea surface temperature: Pacific influence versus local internal variability. *Journal of Climate*, *34*, 2669–2684. https://doi.org/10.1175/JCLI-D-20-0807.1

Zheng, T., Feng, T., Xu, K., & Cheng, X. (2020). Precipitation and the associated moist static energy budget off Western Australia in conjunction with Ningaloo Niño. *Frontiers in Earth Science*, *8*, 1–13. https://doi.org/10.3389/feart.2020.597915

Zhong, A., Hendon, H. H., & Alves, O. (2005). Indian Ocean variability and its association with ENSO in a global coupled model. *Journal of Climate*, *18*, 3634–3649. https://doi.org/10.1175/JCLI3493.1

Zhu, Z. (2018). Breakdown of the relationship between Australian summer rainfall and ENSO caused by tropical Indian Ocean SST warming. *Journal of Climate*, *31*, 2321–2336. https://doi.org/10.1175/JCLI-D-17-0132.1

SUPPORTING INFORMATION

Additional supporting information can be found online in the Supporting Information section at the end of this article.

How to cite this article: Heidemann, H., Cowan, T., Henley, B. J., Ribbe, J., Freund, M., & Power, S. (2023). Variability and long-term change in Australian monsoon rainfall: A review. *WIREs Climate Change*, *14*(3), e823. https://doi.org/10.1002/wcc.823